On the Dynamics of Pedestrians-Induced Lateral Vibrations of Footbridges

Stefano Lenci and Laura Marcheggiani

Abstract. This chapter is concerned with the problem of the large horizontal oscillations induced on slender footbridges by the motion of pedestrians, a phenomenon which involves the synchronization between the motion of walkers and that of the bridge deck. We initially review the extensive technical and scientific literature, and then we focus on two models to detect numerically and analytically the phenomenon. A continuous-time bridge-pedestrians model initially developed by Strogatz et al. is improved to better understand some aspects of the underlying mechanical phenomena. We perform extensive parametric investigations by means of many numerical simulations. This permits to highlight the parameters which mainly affect the trigger and the development of the phenomenon of synchronous lateral excitations, thus allowing a good understanding of the physical event and an evaluation of the engineering reliability of the model. Then, in order to obtain analytical instead of numerical predictions, a nonlinear discrete-time model based on an appropriate 1D map is considered. It is able to provide a reliable value of the number of pedestrians which trigger the synchronization, thus predicting the onset of instability which is also the onset of crowd synchronization. From a dynamical system point of view, the main result is that the model highlights how the phenomenon can be seen as a perturbation of a classical pitch-fork bifurcation, which is then shown to be the underlying dynamical event.

Keywords: Synchronization-induced lateral vibrations, continuous- and discrete-time models, pedestrians-bridge interactions, Millennium Bridge.

Stefano Lenci · Laura Marcheggiani
Department of Architecture, Buildings and Structures, Polytechnic University of Marche, via Brecce Bianche, Ancona, 60131, Italy
e-mail: {lenci,l.marcheggiani}@univpm.it

J. Warminski et al. (Eds.): Nonlinear Dynamic Phenomena in Mechanics, SMIA 181, pp. 63–114.
springerlink.com

1 Introduction and Literature Review

In the last 10–20 years there has been a growing attention toward slender footbridges by engineers and architects, also a consequence of renowned structures, such as the London Millennium Bridge, built by worldwide reputation designers. Often, footbridges are playing a central role in the urban renewal demanded by modern society. It is clear that the beauty and elegance in the architectural concept must spring from simplicity in the structural design, in order to achieve a sort of natural harmony between the fairness of the structure, the physical configuration of the local landscape and the social attractiveness and usefulness of the footbridge. Because of all these social, aesthetic and technical requirements, the trend in footbridge design is towards an increasing flexibility and lightness.

This tendency is supported by the fact that modern materials, thanks to both their mechanical characteristics and their cost competitiveness, allow to consider a high stress level and thus to conceive slender structures with small cross section and large spans.

As a consequence, modern footbridges have small natural frequencies, and possibly have high sensitivity to dynamic loads induced by pedestrians. Excessive vibrations can be caused by resonance between pedestrian loading and one or more natural frequencies of the structure. The reason is that the range of footbridge natural frequencies, both vertical and lateral, often coincides with the dominant frequencies of the pedestrians-induced load [54]: 1.4–2.4 Hz for pedestrian vertical forcing and 0.7–1.2 Hz for pedestrian lateral forcing. It is obvious that if footbridges are designed for static loads only, they may be susceptible to vertical as well as horizontal vibrations, thus confirming the necessity to pay attention to dynamic aspects with a detailed analysis. As a matter of fact, very complex and partially unexpected dynamical phenomena may, and actually do, occur.

Several footbridges experiencing excessive lateral vibrations due to pedestrians-induced loading have been reported in the last years; the most famous is the London Millennium Bridge (a shallow suspension footbridge, Fig.1a) which experienced, on its opening day, strong horizontal vibrations due to the synchronization of the pedestrians motion with the natural modes of the structure [12]–[16]. Other bridges which suffered a similar problem are the Toda Park Bridge (a cable-stayed footbridge, best known as T-Bridge) in Japan [34], [17], the Maple Valley Bridge (a great suspension footbridge, best known as M-Bridge) in Japan [34], the Solferino Footbridge (a double arc steel structure, Fig.1b) in Paris [11] and the Alexandra Bridge in Ottawa [12]. In all these cases, the natural frequency of the principal lateral mode was mainly excited by pedestrians.

We can observe that the problem of the pedestrians-induced lateral vibrations occurred on a range of different structural types (suspension, cable-stayed and steel girder bridges) as well as on footbridges made of different materials (steel, composite steel-concrete and reinforced and pre-stressed concrete) [54]. It is therefore confirmed that a large enough crowd of pedestrians can induce strong lateral vibrations on a footbridge of any structural form as well as of any material, although this

requires the lateral mode to have a low enough natural frequency [12], approximately below 1.3 Hz and close to the range of 0.7–1.2 Hz typical of the pedestrian lateral motion [54].

The theory behind pedestrians-induced lateral vibrations on footbridges is that of synchronous lateral excitation [54], [12], [47]–[14]. People walking in a crowd exhibit a random level of synchrony, and large enough crowds might produce lateral forcing causing a bridge to vibrate laterally. This forcing is the sum of all lateral forces applied to the bridge by the footsteps of each pedestrian. Even if the bridge vibrations are initially very small, pedestrians tend spontaneously to walk in synchrony with the bridge. This ensures an interaction with the bridge for each step of the pedestrians. This instinctive behaviour causes the synchronized pedestrians' footfall forces to be applied at the frequency of the vibration and with a phase such as to increase the motion of the bridge, with each process pumping the other in a sort of *positive* feedback loop [3]; the increase in oscillations amplitude causes pedestrians to increase their lateral footfall forcing and their level of synchrony, by following the movements of the deck in order to balance themselves [12]–[16], [31]: the more the bridge moves, the more the crowd pushes it to move further.

It is recognized from observations that for potentially susceptible spans there exists a critical number of pedestrians that will cause the vibrations to increase suddenly to unacceptable levels. The nature of this problem, in terms of dynamic response of the bridge, is clearly nonlinear (as it is for example confirmed by tests performed on the London Millennium Bridge [12]): the oscillations are small until a critical number of walking pedestrians N_c and then, due to the synchronization, they increase rapidly until a final threshold. This number N_c is of practical engineering interest and its reliable prediction is the final aim of all the theoretical studies.

Several research papers have recently investigated this topic, even if a standard and generally accepted model of pedestrians-induced lateral dynamic loading and of dynamical interaction with the bridge, especially in case of crowding, is missing and

Fig. 1 London Millennium Bridge **a** and Solferino Bridge in Paris **b**: two examples of footbridges undergoing the phenomenon of synchronization induced lateral oscillations

still under research. Zivanovic et al. [54] have performed a comprehensive review of the existing literature on the topic until 2003, while an updated review can be found in [51].

Early studies on pedestrians-induced vibrations of footbridges were carried out at the end of the seventies by Blanchard et al. [6], Matsumoto et al. [29], and Wheeler [53], but they concerned only the measurement and modelling of the vertical component of pedestrian load on a motionless surface. It is worthy to note that Matsumoto and co-workers first attempted to define the vertical dynamic load induced by a crowd and to investigate its stochastic nature, but their approach did not account for interaction with structure and could not describe synchronization.

To model pedestrians-induced lateral vibrations it is necessary to have some understanding of the mechanics which describes human walking, with special attention to the lateral component of the ground reaction force; therefore, some authors (Bauby et al. [4], Belli et al. [5], Vaughan [50], Hof et al. [22], [23], Macdonald [28], Trovato et al. [49]), especially in the area of biomechanical engineering, have recently investigated this topic developing and reorganizing theories on bipedal walking, forcing and frequency of human footfall during walking and balance control. The common observations we can draw from these researches are that: (*i*) locomotion is the translation of the centre of gravity along a pathway requiring the least expenditure of energy; (*ii*) walking biomechanical strategy is to minimize the risk of falling; (*iii*) bipedal locomotion is generated through global real-time entrainment of the neural system on the one hand, and the musculoskeletal system and environment on the other. All these aspects obviously influence the gait pattern and the ground reaction forces in the three directions: vertical, longitudinal horizontal and lateral/transversal horizontal, and are useful to understand what happens when we walk on a laterally moving surface.

Dallard et al. [12]–[16] have conducted a series of controlled crowd tests on the Millennium Bridge and consequently they have proposed a load model based on an empirical observation: during the transient, when bridge wobbling is growing up, the crowd force can be assumed linearly dependent on the lateral oscillation velocity of the deck; this means that pedestrians act like negative damping on the structure. Also a formula has been obtained to evaluate the critical number of pedestrians; it actually depends only on the modal damping of the bridge through a proportionality constant which is strictly related to the specific real case-study (the Millennium Bridge). This phenomenological approach assumes but does not explain the observed synchronization effect, and cannot predict the steady state amplitude for bridge motion, as it is due to not modelled nonlinearities.

Nakamura [33] has proposed an interactive forcing model analogous to the previous one, but which allows the schematization of the self-limiting nature of the synchronization phenomenon and the prediction of the steady state amplitude. Also this model is based on coefficients which have been estimated from experimental tests [34], [17] and cannot easily be generalized to other footbridges.

Newland [36] has approached the problem by referring to the interaction phenomenon between fluid flow and structures which is widely studied in wind engineering (vortex-induced oscillations) and commonly known as lock-in [9], [43].

His model includes the empirical assumption that the 40% of the pedestrians are synchronized with bridge lateral frequency, independently on the amplitude of the oscillations.

Fujino et al. [17] have adopted a model of harmonic forcing by empirically tuning a synchronization parameter for the lateral vibrations of the T-Bridge (according to their experimental data [17]). This model does not predict any sudden transition to a vibrating state of the bridge but assumes a continuous increase in the vibration amplitude as the number of pedestrians increases.

Roberts [38]–[40] has schematized the interaction between the pedestrians and the footbridge assuming that synchronization occurs when the pedestrians motion is larger than the bridge motion; from this critical condition, he obtains a limit number of pedestrians.

Laboratory tests involving a single pedestrian walking on platforms or treadmills forced to move laterally have been carried out by Dallard et al. [12] and McRobie et al. [31] soon after the occurrence of the Millennium Bridge problem.

Ricciardelli and Pizzimenti [41], [42] have recently performed a systematic experimental campaign aimed at characterizing dynamically the lateral force exerted by pedestrians on footbridges, both in case of still deck and in case of laterally moving deck; deterministic and stochastic lateral loading models for the static case have been provided and the bases for more sophisticated dynamic models including crowd-structure interaction have been put. The mechanism of crowd synchronization has been investigated only from the qualitative point of view, deferring its quantitative study and modelling after further future measurements.

Blekherman [7] has explained the excessive lateral vibrations on the Solferino Bridge in Paris on the basis of autoparametric resonance by using a double pendulum model; the process of possible synchronization of pedestrian loading with the relevant vibrational modes, which are nonlinearly coupled in the ratio 2:1 between their frequencies, depends on the achievement of parametric resonance.

Piccardo and Tubino [37] have performed an interesting extensive critical analysis of the excitation mechanisms identified in the literature and they have proposed a new forcing model based on experimental tests carried out on harmonically moving platforms [12], [42]: the force exerted by pedestrians is modelled as harmonic with an amplitude depending on the deck lateral displacement, and a simple criterion defining the limit pedestrian mass is introduced. They mainly ascribe to a mechanism of parametric excitation the lateral sway motion induced by crowds in very flexible, slowly damped footbridges, with a first lateral natural frequency around 0.5 Hz corresponding to a half of the first lateral walking frequency.

Very recently, Venuti et al. [52] have developed a first-order model based on the mass conservation equation, in order to macroscopically describe the dynamics of the crowd in the framework of hydrodynamic modelling: the crowd, considered as pedestrian flow, is assumed to behave like a continuous compressible fluid. The structural system is modelled by means of a generalized single degree of freedom model. The two-way interaction between the crowd and the structure is studied. This model permits to take into account the triggering of the lock-in and its self-limited nature, previously explained only by Strogatz et al. [47]. The effects of two

different kinds of synchronization, i.e. between pedestrians and structure and among pedestrians, are introduced; the presence of different frequency components in the overall force exerted by pedestrians is considered. Some parameters, used in the formulation of the model, come from reasonable qualitative considerations about pedestrian behaviour and they would require specific experimental tests to be confirmed.

Bodgi et al. [8] have adopted a similar approach to simulate the mechanics of synchronous lateral excitation induced by pedestrians on footbridges.

Strogatz et al. [47], [1] have been the first, up to our knowledge, to mathematically describe and predict the simultaneous growth of bridge movement and crowd synchronization, an observation that was unexplained in previous models but that is confirmed by analyses of video footages [2] recorded during overcrowding conditions on lively footbridges [12], [17].

This continuous-time bridge-pedestrians model (called SAMEO in the following) is particularly interesting for its contribution to the physical-mathematical explanation of the underlying mechanical event, besides for the reasonable description of the phenomenon itself. Moreover the model is quite simple in its formulation and general in its application possibilities to any bridge at risk of synchronous lateral excitation; obviously it includes some important simplifications which could affect its predictions from a quantitative point of view. For this reason a consistent detailed analysis can be worthwhile in order to evaluate the engineering reliability of the SAMEO model, and is pursued in the first part of this chapter (Sect. 2).

Due to the large number of nonlinear equations, the analysis is numerical, and is performed by means of a self-made code; extensive parametric investigations are performed through wide numerical simulations and some modifications are introduced with the aim of improving the understanding and the description of the main aspects of the underlying mechanical phenomena. In particular the aim is to give a deeper insight into the synchronization phenomena.

To overcome the limits of a completely numerical analysis, which is accurate but not easy enough for 'immediate' understanding of the involved phenomena, the second main section of the chapter (Sect. 3) is dedicated to present and to analyze in detail a nonlinear discrete-time model which allows to obtain analytical instead of numerical predictions, and to give a dynamic interpretation of the synchronization phenomenon. In this case the approach is therefore analytical by using the classical tools of the discrete nonlinear dynamics.

Some concluding remarks (Sect. 4) about both models end this chapter, which is completely dedicated to the synchronous lateral excitation phenomenon in slender monodimensional civil structures; this is an example of both biological and mechanical synchronization which can be cause of instability.

2 A Continuous-Time Model: The SAMEO Model

The SAMEO model [47]–[14] is able to describe the synchronization of pedestrians motion with the lateral vibrations of footbridges, by adapting ideas originally

developed to explain the collective synchronization of biological oscillators, such as neurons and fireflies, or other nonlinear systems able to phase-lock to an external periodic drive [44], [45]. The basic idea is just the observation that also human walking is governed by unconscious rhythmic biological signals, so an analogy for example with the rhythmic flashing of fireflies seems to be possible.

In the problem we are studying, the stimulus signal is given by the dynamic active feedback between the two involved systems: the bridge and the crowd.

Here lateral synchronization is assumed to involve only one vibrational mode of the structure; this hypothesis is true in *non-pathological* cases in which internal resonance conditions among different natural modes of vibration of the bridge itself do not occur. This is acceptable, e.g., in the London Millennium Bridge case: the analysis of its vertical forces and lateral oscillations shows no correlation between such quantities [12] and so internal resonance is not necessary to explain its lateral sway motion. Moreover the pedestrian lateral excitation is supposed to have a dominant frequency close to the bridge fundamental frequency, as it happens in most of the real observed cases of wobbling footbridges. As a consequence it is sufficient to perform a mono-modal analysis, by projecting the equation of motion of the footbridge on the relevant modal shape.

A footbridge span of length L, measured along the coordinate y, is modelled as a linear mono-dimensional damped dynamical system. To obtain the reduced order, single degree of freedom (SDOF) model, a modal analysis of the whole 3D structure is performed in order to identify the eigenfunction $\varphi(y)$ involving lateral displacements and corresponding to a natural frequency f_0 close to the range 0.7–1.2 Hz typical of the pedestrian lateral excitation. Hence, the dynamics is projected on $\varphi(y)$ and the equation of motion along the selected lateral mode (usually the first) is obtained (Fig.2):

$$M\ddot{X}(t) + B\dot{X}(t) + KX(t) = F_{ped}(t)\,, \tag{1}$$

$$F_{ped}(t) = \int_0^L F_p\,(y,t)\;\varphi\,(y)\,dy \approx G\sum_{i=1}^{N} \sin\Theta_i(t)\,. \tag{2}$$

The overdots denote differentiation with respect to time t. $X(t)$ is the generalized displacement (amplitude) of the relevant lateral mode and M, B, K are the modal mass, damping and stiffness, respectively. $F_{ped}(t)$ is the lateral modal force exerted on the bridge by the pedestrians, projection of the forces on the relevant modal shape, being $F_p(y,t)$ the crowd-induced force per unit length. G is its amplitude and $\Theta_i(t)$ is the phase in the walking cycle for each of the N pedestrians. It is assumed that $\Theta_i = 0$ when the pedestrian's left foot first touches the ground, and $\Theta_i = \pi$ when the right foot is on the ground, interpolating for phases between these events (Fig. 3). According to (2) the pedestrian load is approximated as sinusoidal with respect to the pedestrians phases: it can be thought as the first term in the Fourier series of the (obviously periodic) load function [48].

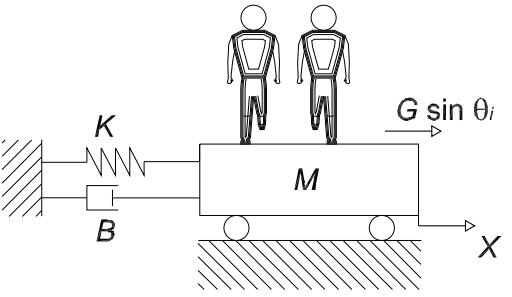

Fig. 2 Mechanical model of the single mode dynamics of the bridge

The dynamical pedestrians-bridge interaction is introduced by assuming that

$$\dot{\Theta}_i(t) = \Omega_i + C_i A(t) \sin(\Psi(t) - \Theta_i(t) + \alpha)\,. \tag{3}$$

Therefore, the pedestrians are considered as limit-cycle phase oscillators with a random distribution of native frequencies Ω_i. C_i measures the pedestrians' sensitivity to bridge lateral vibrations and can be determined experimentally, α is a constant phase lag. It is assumed $\alpha = \pi/2$ in order to match the worst resonance condition in which the instantaneous lateral excitation frequency is approximately equal to the natural frequency of the bridge relevant lateral mode, $\dot{\Theta}_i/\Omega_0 \cong 1$, $\Omega_0 = 2\pi f_0 = \sqrt{K/M}$ being the bridge natural (circular) frequency. $A(t)$ and $\Psi(t)$ are the bridge vibrations amplitude and phase (Fig. 3), which are defined by

$$X = A\sin\Psi,\ \dot{X} = \Omega_0 A\cos\Psi\ \rightarrow\ A = \sqrt{X^2 + \frac{\dot{X}^2}{\Omega_0^2}}\,. \tag{4}$$

The term $f = C_i A \sin(\Psi - \Theta_i + \alpha)$, added to Ω_i in (3), is chosen to be a function of the bridge motion amplitude, of the bridge phase and of the walker phase through a constant of proportionality. It is therefore evident that f has the effect of shifting walkers to a phase closer to that of the bridge, thus modelling the active dynamical bridge-pedestrians interaction and describing the natural tendency of the systems to synchronize. In fact, when the phase difference $(\Psi - \Theta_i + \alpha)$ is positive, i.e. the stimulus is ahead in the cycle (Θ_i lags $\Psi + \alpha$), f is globally positive and the pedestrian speeds up in an attempt to synchronize with the bridge. Conversely, when the phase difference $(\Psi - \Theta_i + \alpha)$ is negative, i.e. the stimulus is behind in the cycle (Θ_i leads $\Psi + \alpha$), f is globally negative and the pedestrian slows down his walking frequency in order to lock to the bridge.

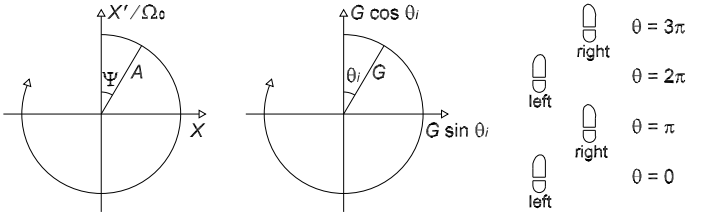

Fig. 3 Definitions of X, A, Ψ and Θ_i

The constant of proportionality, which appears in f, is made of two terms which take into account two different aspects: the effect of the oscillations amplitude and the intrinsic capability of pedestrians to be affected by that amplitude. As A increases, its influence on the pedestrian becomes stronger, according to the linear relationship between f and A. The parameter C_i, on the other hand, quantifies the effect on the pedestrian of the stimulus of amplitude A and phase Ψ , and in this sense it acts like sensitivity to bridge motion.

In the absence of bridge-pedestrians interaction ($C_i = 0$) we have that $\dot{\Theta}_i = \Omega_i$ is the governing equation for the walker dynamics [46], so that each pedestrian walks unconditionally at his own natural constant frequency Ω_i, which has a certain statistical distribution across the population. Then, $\sum_i \sin\Theta_i = \sum_i \sin(\Omega_i t)$ is a distribution with zero mean value, and the bridge is practically still.

In general, from a biological point of view, it is realistic to consider a variation of sensitivity among individuals in the population, and therefore a random distribution of values C_i depending on a person's age, size, health and so on; for sake of simplicity, lacking a specific study in this direction in the literature, in the following it will be used a single constant value for all walkers: $C_i = C$.

Finally it is worthy to note that the model is able to describe the real scenario in which the number of people walking on the bridge deck varies with time: as a new pedestrian enters the bridge, a new equation is added to the system; therefore the number of equations in the model varies with time depending on the number of pedestrians who are entering or leaving the bridge, so that the model can be classified as a time varying system.

2.1 Parametric Investigations: Model Implementation and Computational Aspects

The SAMEO model is governed by highly nonlinear ordinary differential equations; therefore we have to solve them numerically. We use a self-made code which joins

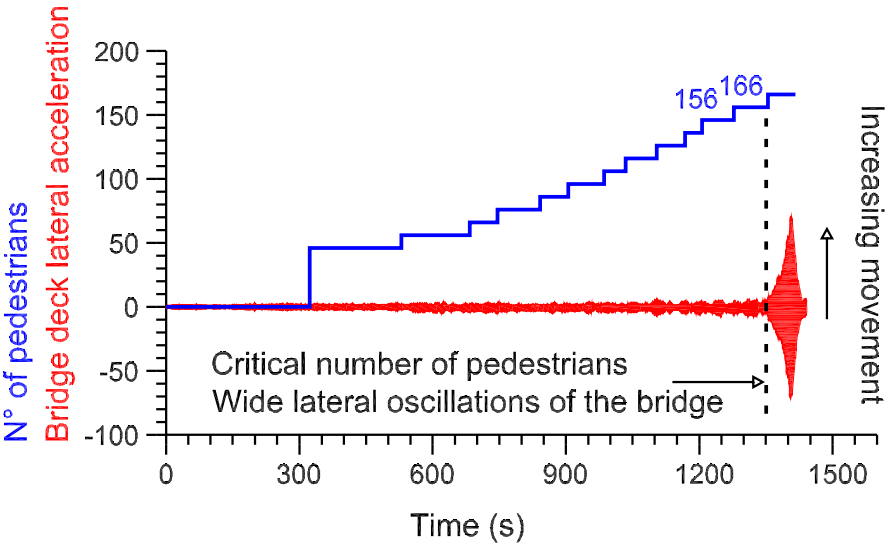

Fig. 4 Results of *in situ* tests on the north span of the Millennium Bridge (Arup figure from [1], [35]): time histories of the number of walkers (staircase-like trace) and of the bridge deck lateral acceleration

traditional numerical methods (the classical routines of Matlab© are used to numerically integrate the system of ODEs (1), (2) and (3) governing the phenomenon) with self-developed algorithms aimed at capturing the main dynamical aspects. Despite the generality of the model, we need data from a real case study and therefore we refer to the Millennium Bridge, as it is the most famous case of wobbling footbridge and also one of the most well-documented and studied in the literature. In fact, in 2000, during its temporary closure, researches were undertaken both through laboratory tests on moving platforms (Imperial College and University of Southampton) and *in situ* tests on the bridge itself (Arup), [12]–[16]. In particular, the latter allowed determining the critical number of pedestrians necessary to destabilize a given span of the bridge, which was found to be about 160 on the north span (Fig. 4).

Because the majority of published experimental data pertains to the fundamental lateral mode of the north span, those numerical values are used as benchmark and reference for our analysis: $M = 113000\,\text{kg}$, $B = 11000\,\text{kg/s}$, $K = 4730000\,\text{kg/s}^2$, which imply $\xi = B/2\sqrt{MK} = 0.0075$ and $\Omega_0 = \sqrt{K/M} = 6.47\,\text{rad/s}$, in turn corresponding to 1.03 Hz. Furthermore, according to [47], we assume $G = 30\,\text{N}$, $C_i = C = 16\,\text{m}^{-1}\,\text{s}^{-1}$ and, as said, $\alpha = \pi/2$.

We adopt for the native frequencies Ω_i a Gaussian distribution (Fig. 5a) with mean value 1.03 Hz (6.47 rad/s) and standard deviation 0.1 Hz (0.63 rad/s) [54]. The initial phases (Fig. 5b) are supposed uniformly distributed in the interval $[0, 2\pi]$. We choose these phases randomly with the idea to reproduce the different moments when each new individual enters the footbridge; these random constants are used

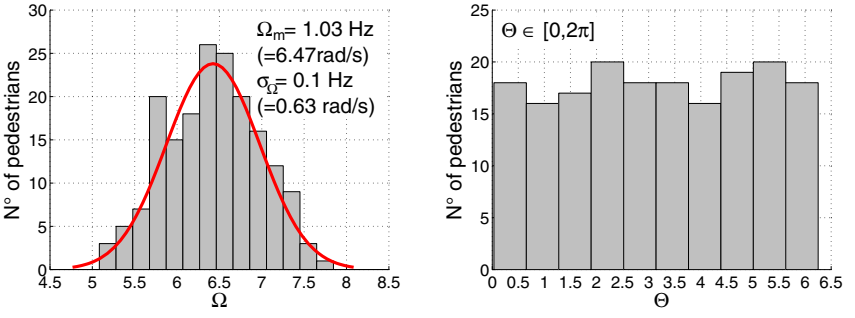

Fig. 5 Distribution of **a** native frequencies Ω_i and **b** initial phases Θ_i for a generic group of 180 pedestrians considered in our simulations

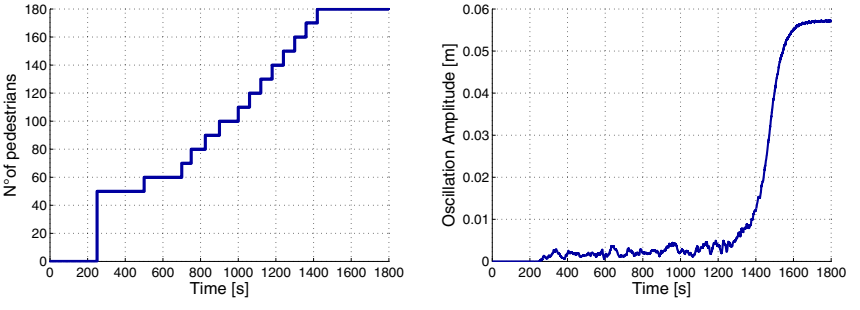

Fig. 6 Number of walkers on the bridge **a** and amplitude of vibration **b** versus time

exclusively as initial conditions for numerically integrate the system of ordinary nonlinear differential equations in the Monte Carlo simulations.

The initial position and velocity of the bridge are zero. Fig. 6 shows the pedestrians ramp and a typical plot of the oscillation amplitude: we consider a staircase loading path in order to reproduce Arup test conditions on the Millennium Bridge (see the upper staircase-like trace in Fig. 4) and the relevant results (see the lower trace in Fig. 4).

For small crowds, the oscillation amplitude (Fig. 6b) as well as the bridge deck lateral acceleration (Fig. 4) is near zero, with a fluctuating trend, as walkers are still desynchronized and randomly phased. Then, as more and more people walk on the deck, there is no hint of instability until the crowd reaches a critical size N_c, after that wobbling and synchrony suddenly emerge simultaneously, as dual aspects of a single instability mechanism.

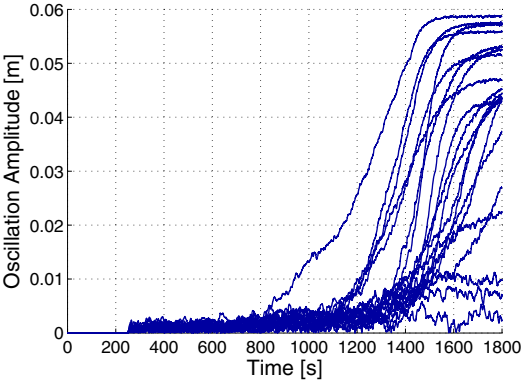

Fig. 7 Amplitude of vibration versus time for a first group of 20 simulations

The practical estimation of N_c from our simulations is made by an *ad hoc* numerical procedure based on the identification of the onset time for the exponential growth of the instability t_c (see the following subsection 2.1.1): from the generic amplitude versus time curve (Fig. 6b), we determine this critical threshold t_c, then with this value we enter the staircase loading path graph and we read the corresponding critical number of pedestrians N_c triggering the synchronization.

For the reference case we perform a Monte Carlo analysis with 200 simulations; the results, in terms of crowd's critical size N_c, are randomly distributed: we evaluate its mean value $N_a = 155$ and its standard deviation $\sigma_N = 27.7$. Our critical number is practically coincident with the Arup's results, and the predicted final amplitude of the bridge motion is very close to the observed values of about 5–7 cm on the opening day. For a reason of graphic readability we plot in Fig. 7 only a sample of 20 simulations, which is in any case visually representative of the global outcome of the whole group of 200.

From Fig. 7 it clearly emerges that, despite the loading path is the same for all the simulations, the response in terms of amplitude changes significantly: even if in most simulations pedestrians synchronize, there are also some cases in which they synchronize a little and others (only 3 in the sample of 20 simulations reported) in which pedestrians do not synchronize at all in the considered time interval. The variations from one run to the next depend on the initial values of Θ_i and on Ω_i, randomly assigned (Fig. 5) to pedestrians at each simulation; the consequence is a dispersion of the critical values N_c, as confirmed by the quite large standard deviation ($\sigma_N = 27.7$).

The results of Fig. 7 constitute the reference case with respect to which we develop all the subsequent analysis.

In the following we perform 200 simulations for each tested case, in order to obtain statistically reliable considerations, even if, as before, for readability reasons we always plot only a sample of 20. For each group of simulations, the average N_a and the standard deviation σ_N of the critical numbers N_c are computed: they summarize the outcome of the performed investigations.

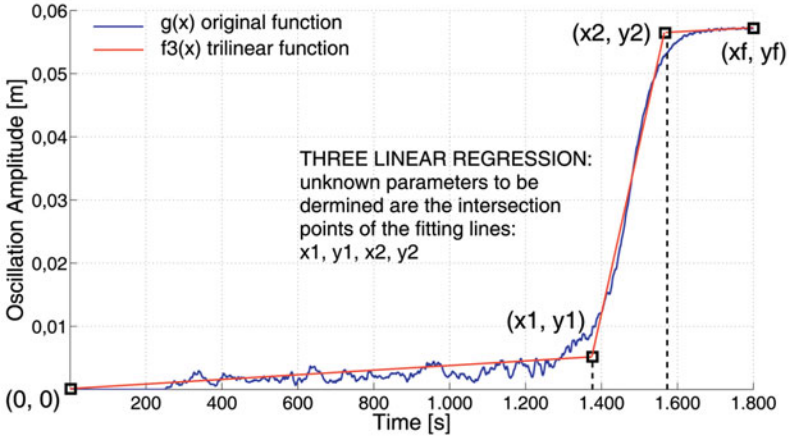

Fig. 8 Multi-phase linear regression: data points are divided into 3 segments on the x axis and then a different straight line is fitted to each segment; the intersection points are not known *a priori*

In order to perform an extensive parametric analysis, which is one of the aims of this section, it is necessary to automate as much as possible the computation of N_a and σ_N. This is done in the next subsection.

2.1.1 Automatic Detection of N_c

To automatically detect the time t_c for the onset of the instability, and consequently the critical number N_c of pedestrians triggering the unwanted dynamical phenomena, we develop a numerical technique to fit the oscillations amplitude versus time curve, $g(x)$, by a piecewise linear averaging curve. Actually, we use three straight segments (Fig. 8), which are sufficient for our purposes. In fact, by observing the SAMEO model results (Fig. 6 and Fig. 7), we can clearly identify three different ranges, in each of them the data points having an approximately linear trend. This three-linear regression is not so trivial, because it is, in fact, a nonlinear regression problem due to the two unknown intersection points of the fitting segments; the problem is continuous but not differentiable at those points and this messes up the local linearization approach often used for weakly nonlinear problems. In particular, here we are interested in finding the intersection point between the first and the second segment, as it corresponds to a reliable and automatic estimate of t_c and therefore, from the load path, of N_c.

The goal is to approximate our real rippled function $g(x)$ with a *tri-linear* function $f^{(3)}(x)$ defined as follows (Fig. 8):

$$f^{(3)}(x) = \begin{cases} \dfrac{y_1}{x_1} x, & \text{for } x < x_1, \\ y_1 + \dfrac{y_2 - y_1}{x_2 - x_1}(x - x_1), & \text{for } x_1 < x < x_2, \\ y_2 + \dfrac{y_f - y_2}{x_f - x_2}(x - x_2), & \text{for } x_2 < x. \end{cases} \tag{5}$$

We fix the first and the last point, respectively $(0,0)$ and (x_f, y_f), as those of $g(x)$, so in Eq.(5) the unknown parameters are the four coordinates of the two intersection points of the fitting lines: x_1, y_1, x_2, y_2. We determine them by minimizing the total quadratic error between the original curve and our piecewise linear approximation:

$$\varepsilon(x_1, y_1, x_2, y_2) = \int_0^{x_f} \left(g(x) - f^{(3)}(x) \right)^2 dx \propto \sum_{i=1}^{M} \left(g\left(x^{(i)}\right) - f^{(3)}\left(x^{(i)}; x_1, y_1, x_2, y_2\right) \right)^2 . \tag{6}$$

We underline that in the previous Eq. (6) we pass from the rigorous integral definition of total quadratic error to a discrete formulation, by simply integrating with the trapeziums rule: M is the number of points, equally spaced in time, in which we discretize the time-history. In the right hand side of (6) we omit to multiply for the constant integration interval Δx because, when we minimize, it does not affect the minimum *point* we are looking for.

To minimize the function ε with respect to the parameters x_1, y_1, x_2 and y_2 we use the simplex method of Nelder and Mead [26], [18], which is a direct method that does not use numerical or analytic gradients. From any 'initial' guess of x_1, y_1, x_2 and y_2 the algorithm runs and provides a 'minimum' of the function. In our case the parameters to initialize are only x_1 and x_2 since for sake of simplicity we choose as initial guess $y_1 = g(x_1)$ and $y_2 = g(x_2)$. For particular situations the algorithm can fail to converge or converge to a *local* minimum. When the *global* minimum is not achieved, we solve the impasse by automatically (and randomly) changing the initial guess. To improve the reliability of the results, we consider in any case different initial guesses even when the solution does not show drawbacks.

This procedure, despite the thousands of function evaluations to determine the optimum, is computationally efficient, and it takes only few seconds to give the result. This aspect can be further improved if we filter the input data with a lowpass filter and then resample the resulting smoothed signal at a lower rate; with this trick we are also able to reduce the problem connected with multiple local minima. In any case, for each group of simulations, a global visual supervision of the plotted results is required in order to be sure of the correct prediction of N_c. In this sense our code does not permit completely automated results.

Despite this limit, the method we use is able to detect in a sufficiently automatic manner the number of pedestrians which trigger the synchronization, and it allows us to perform a wide set of simulations with an acceptable CPU time, thus deriving statistically reliable considerations.

2.2 Numerical Simulations

We perform extensive parametric investigations with the following practical motivations:

1. to test the robustness of the model;
2. to improve the understanding of some aspects of the underlying mechanical phenomena (e.g. to give a deeper insight into the synchronization phenomena);
3. to increase the agreement of the model results to the effective behaviour of the walkers, as observed in real conditions;
4. to highlight the role of the main parameters involved on the system dynamics.

We choose as parameters to be varied those which mainly affect the model behaviour and which are sensitive with respect to the real situation to be modelled:

1. the initial phases and native frequencies for the walkers;
2. the constant phase-lag parameter α;
3. the amplitude of the pedestrian lateral forcing during walking;
4. the shape of the pedestrian loading wave;
5. the pedestrians' sensitivity to the bridge motion, C;
6. the coherence of the model results with respect to an 'inverse' approach analysis;
7. the synchronization between pedestrians, D (to be introduced later);
8. the interaction between the two types of synchronization, through the tuning of the respective parametric indicators C and D;
9. the effects of different loading paths, i.e. different modality and number of pedestrians introduced on the bridge deck per unit time.

We remark that we also introduce and test some modifications to the original SAMEO model, maintaining unaltered its essence and plainness of description of the physical event but improving its effectiveness. Our enhancements concern:

1. the addition of a further level of synchronization, between pedestrians;
2. a different, and more conservative, relationship between the amplitude of the pedestrian lateral forcing and the amplitude of the bridge lateral vibrations, which we determine according to experimental tests [12];
3. a more realistic square-type shape of the pedestrian loads on the bridge, according to experimental evidences on treadmill [5].

2.2.1 Influence of Pedestrians Initial Phases and Native Frequencies

What happens if the pedestrians enter the bridge with some initial level of synchrony, as it may occur in overcrowding conditions, or if they are a typologically homogeneous group with native frequencies slightly spread around the mean value?

In Fig. 9 we analyze the influence of the initial conditions of the walkers on the temporal course of the phenomenon: we assign random phases Θ_i uniformly distributed in an interval $[0,1]$ instead of $[0,2\pi]$ (see for comparison Fig. 5b), and

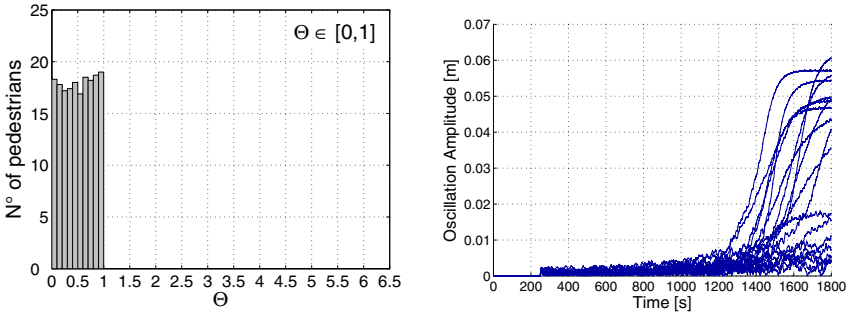

Fig. 9 Effect of the initial level of synchrony among pedestrians: **a** phases distribution and **b** amplitude of vibration versus time curves

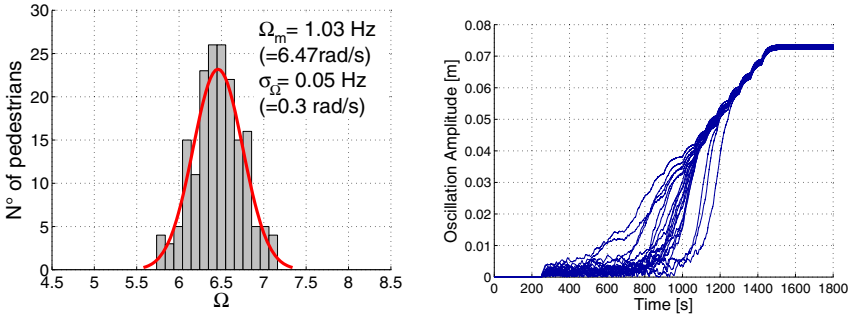

Fig. 10 Effect of the typological homogeneity level of the pedestrians: **a** native frequencies distribution and **b** amplitude of vibration versus time curves

we keep all the other parameters unchanged with respect to the reference case. This entails to admit an initial synchrony among pedestrians.

With these initial conditions, we obtain wobbling for an almost identical critical value, $N_a = 160$, which is affected by a similar dispersion, $\sigma_N = 24.32$. On the other hand, if we compare the amplitude of vibration versus time curves reported in Fig. 9b with those of the reference case (Fig. 7), we observe that substantial differences do not exist. Here pedestrians enter the bridge next to the synchrony, so their initial behaviour is less random than the previous one (Fig. 5b); but the point is that they are synchronized among them, not with the bridge. Therefore, as they have different native frequencies, after one step they will not be anymore synchronized, and the phenomenon will proceed almost as in the reference case.

In Fig. 10 we analyze the influence of the intrinsic properties of the pedestrians: we assign random native frequencies according to a Gaussian distribution with the same mean value (6.47 rad/s), but with a smaller standard deviation ($\sigma_\Omega = 0.3$ rad/s instead of 0.63 rad/s) and we keep all the other parameters unchanged with respect to the reference case.

In general walkers tend to have a natural frequency of pacing that varies depending on the height and weight of the individual, on his/her age, on the travel purpose, on physical, social and psychological factors. Here we suppose that an almost homogeneous group of pedestrians enter the bridge; this means they have natural frequencies near the mean value for the population (1.03 Hz), which is near the bridge resonant frequency. It is obvious that, in such situation, the synchrony with the bridge lateral movements is fostered and sped up. In fact, as expected, we obtain wobbling for a quite smaller critical value, $N_a = 84$, which is affected by a smaller dispersion, $\sigma_N = 15.69$. By observing the amplitude of vibration versus time curves (Fig. 10b), we highlight that, unlike the other cases (Fig. 7 and Fig. 9), in all the simulations pedestrians synchronize in a quite restricted time scale, inside the considered time interval.

Since the reduction from $N_a = 160$ (Fig. 9b) to $N_a = 84$ (Fig. 10b) is very marked, we conclude that the typological homogeneity degree of the crowd is a determining factor both for the trigger point of instability and for the temporal probability of the event to occur, while the initial level of synchrony among pedestrians does not affect the onset of the phenomenon.

2.2.2 The Constant Phase-Lag Parameter α

The constant phase-lag parameter α is determined by a pedestrian's desired phase relationship with the moving surface. It is recognized that on a laterally moving surface, the generic walking pedestrian tends to counterbalance the oscillations with a snaking gait: this instinctive behaviour fosters the bridge lateral vibrations.

If we observe the typical variation of the dynamic amplification factor (DAF) and of the phase angle (ϕ) as a function of the frequency ratio $\beta = \dot{\Theta}_i/\Omega_0$ (see Fig. 11), we note that $\alpha = \pi/2$ gives the worst-case scenario in which the bridge is maximally destabilized because pedestrians drive it most 'efficiently', so that the resulting prediction of the critical number of walkers is conservative. On the contrary $\alpha = 0$ corresponds practically to the 'static' case ($DAF = 1$) in which the synchronized pedestrians are not effective in applying their force and in amplifying bridge oscillations. Therefore $\alpha = \pi/2$ is the correct value for human response to lateral vibrations.

To confirm the previous interpretation we have reported in Fig. 12 the results obtained for $\alpha = 0$. We can observe that the bridge lateral vibrations remain in the field of the little oscillations (in the order of mm): pedestrians are not able to trigger wide lateral oscillations of the bridge, not even if we consider a longer time of observation under the same maximum final value of pedestrian loading (Fig. 13).

2.2.3 Pedestrian Forcing Amplitude

In the previous simulations we have assumed G to be a constant independent of A, i.e. independent of how much the bridge is wobbling. Its value (30 N) corresponds to the mean amplitude of the lateral force by an average pedestrian during normal walking,

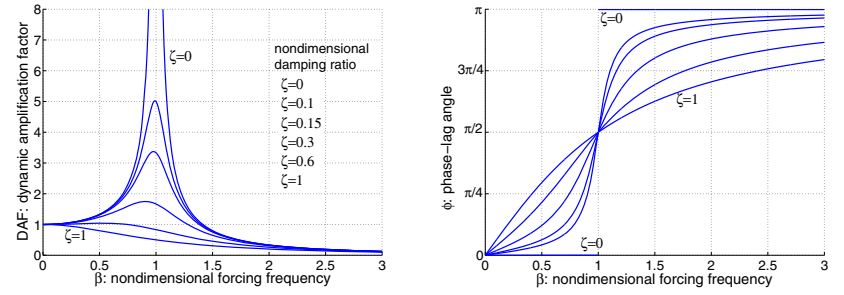

Fig. 11 Variation of dynamic amplification factor ($DAF = 1/\sqrt{(1-\beta^2)+4\zeta^2\beta^2}$) **a** and of phase angle ($\phi = \arctan(2\zeta\beta/(1-\beta^2))$) **b** with damping ($\zeta$=0, 0.1, 0.15, 0.3, 0.6, 1) and frequency (β), for a single d.o.f. damped oscillator harmonically excited

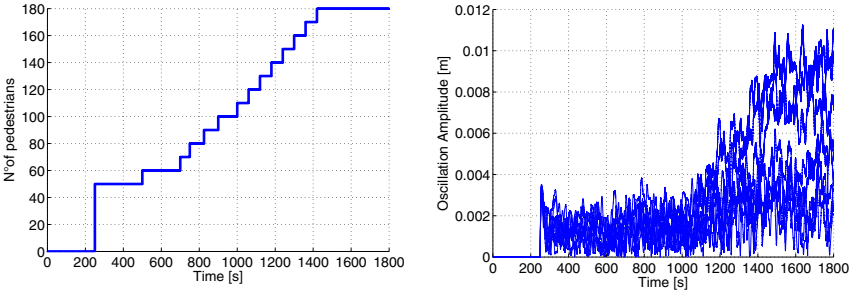

Fig. 12 Number of walkers on the bridge **a** and amplitude of vibration **b** versus time for $\alpha = 0$

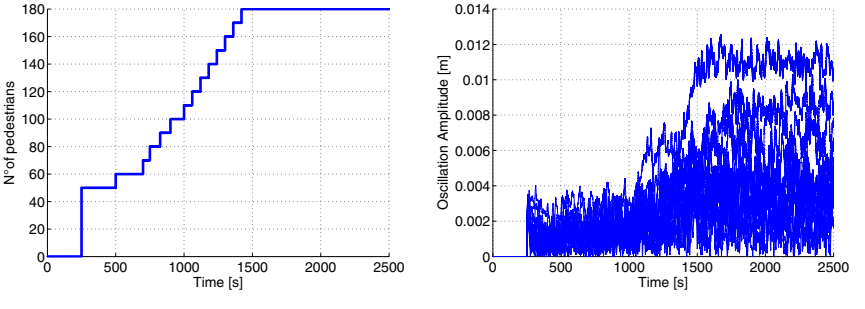

Fig. 13 Number of walkers on the bridge **a** and amplitude of vibration **b** versus time for $\alpha = 0$; a longer time of observation under the same maximum final number of pedestrians is considered here

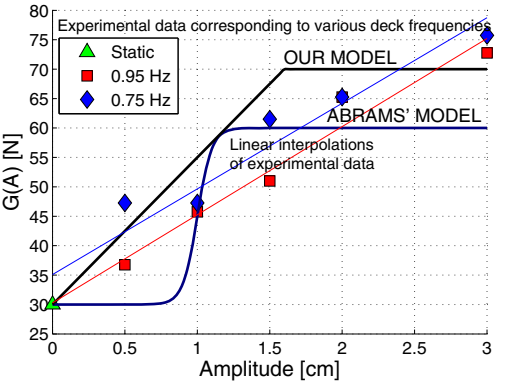

Fig. 14 Lateral forcing amplitude versus bridge vibration amplitude (gait function): experimental data by Arup obtained at the London Imperial College tests (dots), Abrams' model (7) and our model (8)

as experiments on a treadmill confirm [5]. It is known that the magnitude of this force can increase when the pedestrian is on a laterally moving surface, because he widens his stance and adopts a different gait in order to balance himself [12], [31], [4].

We consider this effect of changing gait by assuming a model of pedestrian force proposed by Abrams [1] and motivated by the experiments of McRobie et al. [31] (Fig. 14):

$$G(A) = (1/2)\left(G_{low} + G_{high}\right) + (1/2)(G_{low} - G_{high}) \tanh\left[C_2\,(A - C_1)\right]. \quad (7)$$

Here $G_{low} = 30\,\mathrm{N}$ and $G_{high} = 60\,\mathrm{N}$ are the minimum and the maximum forcing amplitude; $C_1 = 1\,\mathrm{cm}$ and $C_2 = 10\,\mathrm{cm}^{-1}$ are the amplitude at which the force increases, and the rate at which the force increases with the oscillation amplitude, respectively [1].

Numerical results show that in this case the amplitude curves lift off for a number of pedestrians, $N_a = 150$, slightly smaller than that corresponding to constant G, but the standard deviation is strongly reduced, $\sigma_N = 14.65$. Moreover, it is interesting to note that the maximum final value of A is higher (14 cm against about 7 cm in the reference case), according to the fact that the model is linear in the mechanical part. We can then affirm that doubling G when oscillations reach only 1.3 cm, as it happens with the expression (7), see Fig. 14, has the effect of doubling the bridge final oscillation amplitude and of reducing the dispersion, while it does not affect significantly the instability critical threshold (Fig. 15a).

We also implement a different and more conservative bilinear function $G(A)$:

$$G(A) = \begin{cases} 30 + 2500A, & \text{for } A \le 0.016\,\mathrm{m}, \\ 70, & \text{for } A > 0.016\,\mathrm{m}. \end{cases} \quad (8)$$

This expression is chosen in order to overlay, for sake of security, the greatest possible number of laboratory tests' data [12], as shown in Fig. 14. The simulations provide a fairly lower critical number of pedestrians, $N_a = 130$, and a larger standard

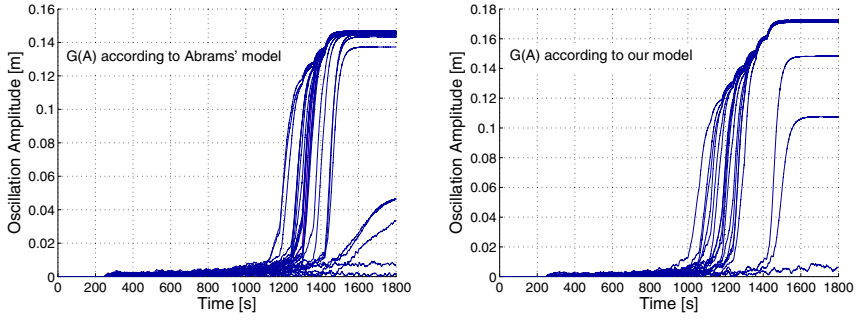

Fig. 15 Amplitude of vibration versus time: simulations performed with $G(A)$ according to **a** Abrams' model and **b** our model

deviation, $\sigma_N = 24.28$, according to the fact that the force applied to the bridge is higher with respect to Abrams' gait function (7). The same considerations of Eq. (7) apply to the maximum final value of A (Fig. 15b).

Both the models assume $G(A)$ increasing, more or less rapidly, until a certain saturation threshold and then constant (Fig. 14); this trend is motivated by the observation that both the magnitude of the pedestrian lateral forcing and the phenomenon itself are naturally self-limiting: in fact a human sensitivity limit to lateral vibrations exists, after which pedestrians begin to have difficulty in walking and finally stop.

From Fig. 15 we also observe that incorporating in the model the dependence $G(A)$, with both the Eqs. (7) and (8), speeds up the time scale for the growth of bridge oscillations towards the steady state, after the critical crowd size has been exceeded.

2.2.4 Pedestrian Forcing Shape

In the original SAMEO model the pedestrian force is idealized as sinusoidal (2), even though experiments on treadmill reveal a periodic trend more similar to a square wave [5] (Fig. 16):

$$F_{ped,i} = G\,\mathrm{sign}\,(\sin\Theta_i)\ . \tag{9}$$

Our simulations show that in the case of square-type force (9), the phenomenon triggers for a number of pedestrians $N_a = 125$, smaller than that of the sinusoidal wave case, while the standard deviation practically does not vary, $\sigma_N = 24.55$. The maximum final value of A is fairly higher: about 8 cm (Fig. 17).

This behaviour was expected as for the square wave a higher force is applied to the bridge (on the average the force is 1.41 times larger, since $\int_0^{2\pi}[\sin(\Theta_i)]^2 d\Theta_i = \pi$ while $\int_0^{2\pi}[\mathrm{sign}(\sin(\Theta_i))]^2 d\Theta_i = 2\pi$), thus strengthening the 'positive' feedback loop between synchrony and wobbling.

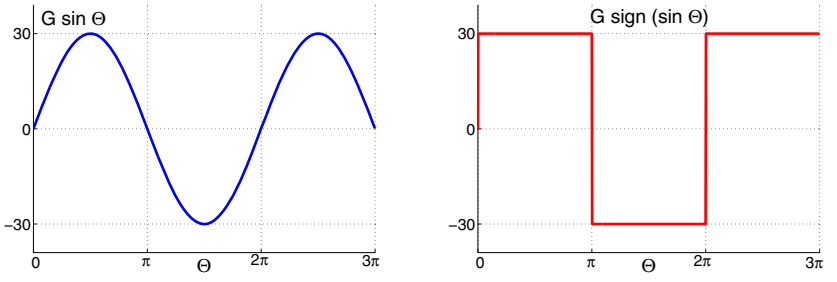

Fig. 16 Pedestrian lateral forcing: **a** sinusoidal and **b** square-wave

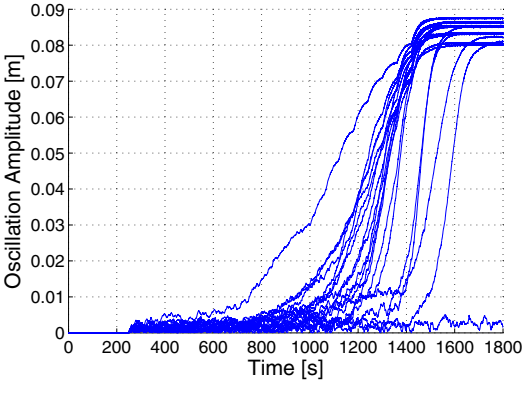

Fig. 17 Amplitude curves obtained in the case of square-type force

We can then conclude that the temporal shape of the pedestrian force plays a more important role than the variation of G with A, being the decrement in the critical crowd size more marked. Therefore, the square wave force shape is both more realistic and more safe.

2.2.5 Pedestrian Sensitivity to Bridge Motion

The parameter C controls how fast a pedestrian, unconsciously, shifts the phase of his walking cycle in response to the sideways oscillations of the platform on which he is walking. There are both physical (related to its meaning of pedestrian sensitivity) and mathematical reasons (related to its definition in (3)) to assume that C is positive; in fact, since A is positive, the sine function in (3) is already able to alter the instantaneous pedestrian frequency in the desired way, i.e. slowing down the pedestrian if he is walking too early with respect to the bridge or speeding up him otherwise.

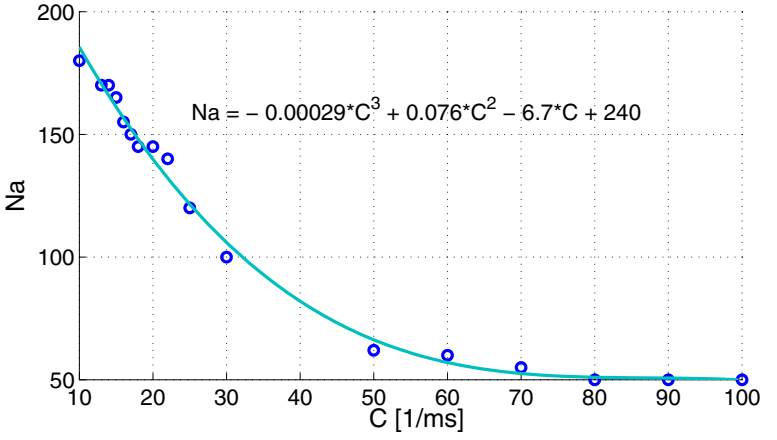

Fig. 18 Average critical number of pedestrians versus C: data points and fitted cubic curve

Apart from the previous one, we have no other overall information on C. In fact, being the parameter which, in some sense, links the mechanical behavior of the bridge, governed by the laws of the physics, with the human behavior of pedestrians, which is not subjected to well-known and mathematically established governing law, C is the most delicate parameter of the model, and actually the most difficult to be determined; practically, it cannot be determined directly, but only indirectly by comparing experimental and model outcomes. For this reason it is very important to perform a parametric analysis with respect to C or, more precisely, to determine how N_a depends on C, beyond the value $C = 16\,\mathrm{m^{-1}s^{-1}}$ suggested by [47].

In Fig. 18 we report the average critical number of pedestrians corresponding to values of C in the range $10 - 100\,\mathrm{m^{-1}s^{-1}}$: each point in the graph is the result, as usual, of 200 simulations performed considering Arup loading path. The best (in the least squares sense) cubic curve fitting the data is:

$$N_a = -2.9 \times 10^{-4} \times C^3 + 7.6 \times 10^{-2} \times C^2 - 6.7 \times C + 240\,. \tag{10}$$

Values of $C < 10\,\mathrm{m^{-1}s^{-1}}$ are investigated but they are not plotted in Fig. 18, because in these cases the pedestrians are never able to synchronize and only small oscillations are observed. In Fig. 19a we show a sample of 20 of the 200 simulations performed with $C = 10\,\mathrm{m^{-1}s^{-1}}$: in only one case the system seems to be able to synchronize in the considered time interval. In general only carrying forward the simulations for unrealistically high values of time and number of pedestrians, synchronization is a possible outcome. Thus, $C = 10\,\mathrm{m^{-1}s^{-1}}$ can be assumed as a lower bound for the human sensitivity parameter to bridge lateral vibrations.

Going forward, values of C up to $14\,\mathrm{m^{-1}s^{-1}}$ are of little practical interest as the trigger of the phenomenon is still characterized by great uncertainty and only some samples synchronize.

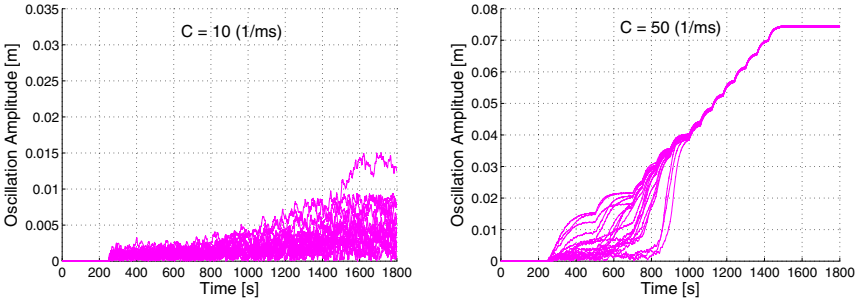

Fig. 19 Amplitude of vibration versus time: **a** curves obtained with $C = 10\,\mathrm{m^{-1}s^{-1}}$ and **b** with $C = 50\,\mathrm{m^{-1}s^{-1}}$

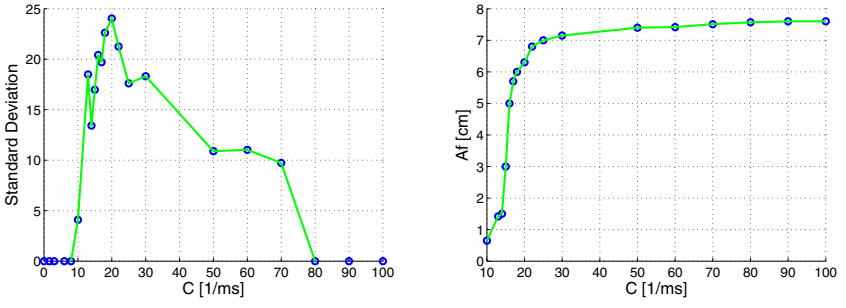

Fig. 20 Standard deviations **a** and maximum final amplitude of bridge vibrations **b** associated to the mean values of the pedestrians critical number triggering the synchronization: simulations performed by varying C

Overall as C increases, the critical crowd size decreases (Fig. 18) and the maximum final amplitude of the bridge oscillations increases (Fig. 20b). Then, for values of $C > 50\,\mathrm{m^{-1}s^{-1}}$, the critical threshold keeps almost identical: synchronization instantly occurs, when only the first loading step of 50 pedestrians is applied on the bridge. This means that $C = 50\,\mathrm{m^{-1}s^{-1}}$ can be assumed as an upper bound for the human sensitivity parameter to bridge lateral vibrations. In Fig. 19b we show the result of simulations performed with $C = 50\,\mathrm{m^{-1}s^{-1}}$ ($N_a = 60$ and $\sigma_N = 10.89$).

Thus we clearly define the limits for the pedestrians-bridge synchronization parameter C: values lower than $10\,\mathrm{m^{-1}s^{-1}}$ and higher than $50\,\mathrm{m^{-1}s^{-1}}$ are not meaningful; we highlight that the range of most practical interest is for $C \cong 14 - 25\,\mathrm{m^{-1}s^{-1}}$, as these are the most realistic values of pedestrian sensitivity (this range includes $C = 16\,\mathrm{m^{-1}s^{-1}}$, value for which the model results match the experimental data for the north span of the Millennium Bridge) and also the most delicate (in this range the average critical number N_a decreases more quickly, see Fig. 18).

For completeness of investigation, in Fig. 20a we report also the standard deviation σ_N associated to the mean value N_a of the critical number of pedestrians, for each group of simulations performed by varying C. If we neglect the irregularities

of statistical nature, we can observe that σ_N starts from zero, follows an increasing trend until a peak threshold for $C \cong 14 - 25\,\mathrm{m^{-1}s^{-1}}$ and then decreases again to zero. A possible interpretation is that the more the pedestrians are sensitive to bridge lateral vibrations, the more the initial values of phases and native frequencies, randomly assigned at each simulation, influence the temporal evolution of the phenomenon in terms of results dispersion; as a consequence the critical threshold N_a is affected by an increasing standard deviation, and this trend is maintained until the peak threshold. Then when the sensitivity increases beyond that range, a trend reversal occurs: pedestrians are so sensitive to bridge lateral vibrations that they are progressively less and less influenced by the initial conditions, and the critical threshold N_a is affected by a standard deviation which drops to zero. Therefore $C \cong 14 - 25\,\mathrm{m^{-1}s^{-1}}$ is also the range in which the initial conditions are mainly able to influence the phenomenon, with a resulting higher dispersion in our prediction of N_a. In addition, we observe that the maximum final amplitude of the bridge oscillations increases rapidly in this range before reaching a plateau (Fig. 20b).

These considerations confirm that $C \cong 14 - 25\,\mathrm{m^{-1}s^{-1}}$ is the most critical range of values for C, and therefore our interest will be concentrated on it (see the following subsection 2.2.8).

2.2.6 Inverse Approach Analysis: Coherence of the Model Results

With reference to the specific example of the Millennium Bridge, it may be interesting to analyse also an 'inverse' approach in the evaluation of the model behaviour. Instead of investigating what happens to the crowd critical size when we vary the model parameters or the description of the pedestrian load, we can study which is the value of C able to give a model critical threshold coinciding with the experimental one. Actually, this is the way with which C can be determined for each 'variant' of the SAMEO model.

With this aim we perform simulations by looking for the value of C such that $N_a = N_{c,exp}$, when:

1. G is assumed variable with the bridge oscillation amplitude according to Eq. (7) (see the following Fig. 21);
2. the pedestrian force is assumed of 'square-type' according to Eq. (9), instead of sinusoidal (see Fig. 22 hereunder).

In this first case, if we compare our simulations results with data obtained from crowd tests on the Millennium Bridge [12], we confirm the value $C = 16\,\mathrm{m^{-1}s^{-1}}$ obtained with $G = \text{constant} = 30\,\mathrm{N}$. This is not surprisingly, since in the subsection 2.2.3 we have shown that with (7) N_a is only slightly smaller than that corresponding to $G = 30\,\mathrm{N}$ (150 vs 155), the difference being hidden by the statistical nature of the problem.

In this second case, in order to match the model predictions to the Arup experiment, the correct value for C is slightly smaller: $15\,\mathrm{m^{-1}s^{-1}}$. This is a reasonable result as in this case we put suddenly more energy into the system and therefore, in order to obtain the same response of the reference case, we have to consider a

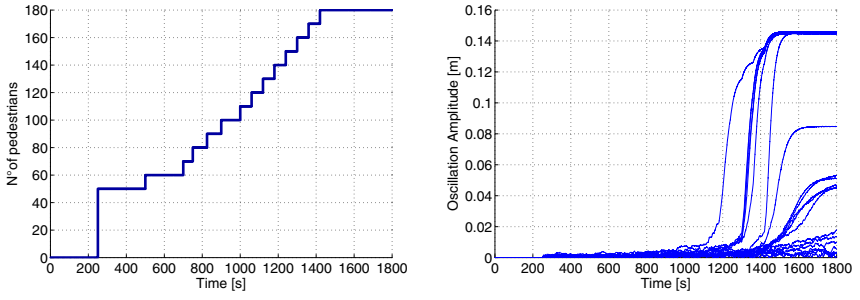

Fig. 21 Number of walkers on the bridge **a** and amplitude of vibration **b** versus time when G is variable with A according to Abrams' model (7). Simulations performed with $C = 16\,\mathrm{m}^{-1}\mathrm{s}^{-1}$

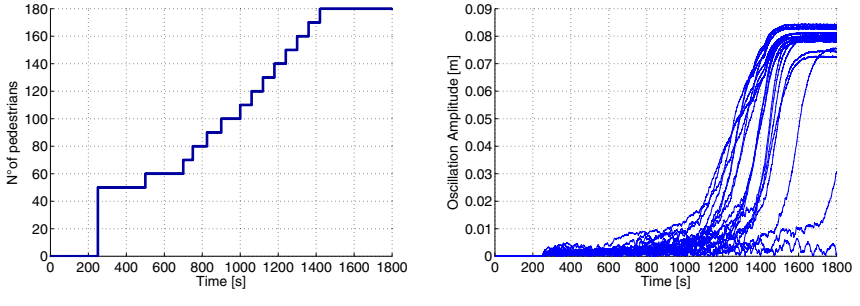

Fig. 22 Number of walkers on the bridge **a** and amplitude of vibration **b** versus time when the pedestrian force is assumed of 'square-type' instead of sinusoidal (9). Simulations performed with $C = 15\,\mathrm{m}^{-1}\mathrm{s}^{-1}$

lower value of the sensitivity parameter. These results are in full agreement with those obtained in subsection 2.2.4, where for the case $C = 16\,\mathrm{m}^{-1}\mathrm{s}^{-1}$ and with a 'square-type' pedestrian force, we had obtained a fairly lower critical number N_a.

Overall the SAMEO model seems to provide coherent results with respect to an inverse approach analysis, in spite of the statistical data involved in its predictions.

2.2.7 Synchronization between Pedestrians

The original formulation of the SAMEO model considers only the bridge-pedestrians interaction, and not an interaction between pedestrians. Since it was found that a certain level of synchronization among people within the crowd exists [54], [20], it should be considered also a correlation due to people falling into step with each other, simply responding to visual clues such as the movement of people in front of them [25]. There is experimental evidence that the brain's control center syncs

up to its visual center with high-frequency brain waves, directing attention to select features of the visual world [19]. In a crowded bridge, lacking other external stimuli, human attention is caught by the people who are walking ahead, with a tendency to synchronize in order to minimize the reciprocal interferences and to achieve a more comfortable and fluent gait [32]–[24].

To describe this phenomenon we add to the SAMEO relation for the bridge-pedestrians interaction (3) a term which takes into account the pedestrian- to- pedestrian interaction. However, without complicating too much the model, we consider that a pedestrian interacts only with the one who is in front of him (Fig. 23), who is the one who mainly influences his motion. From a practical point of view, this means to consider pedestrians walking 'in single file' (i.e. lined up one behind another): this is obviously a simplification of the real crowd interaction, although it exactly corresponds to the Arup experiments on the Millennium Bridge [2]. It can be considered as a rough preliminary proposal and additional features could be dealt with after a fundamental understanding has been established. Indeed our modified SAMEO model is very flexible in its present form, and the real effect on the single individual of all the pedestrians who are ahead in his/her visual cone could be easily introduced through an 'average effect coefficient', determinable with proper experimental analyses of human behavior.

Instead of (3) we then assume:

$$\dot{\Theta}_i = \Omega_i + C_i A \sin(\Psi - \Theta_i + \alpha) + D_i \sin(\Theta_{i-1} - \Theta_i)\,. \tag{11}$$

The new term $g = D_i \sin(\Theta_{i-1} - \Theta_i)$ is chosen in analogy with the bridge-pedestrians interaction term and on the basis of the following considerations:

1. it is a function of the phase difference between pedestrians 'in single file', being Θ_{i-1} the phase of the generic leading pedestrian $i-1$ which acts as stimulus signal for the following pedestrian i walking just behind;
2. it has the effect of shifting each walker to a phase closer to that of the previous one. Therefore, when the phase difference $(\Theta_{i-1} - \Theta_i)$ is positive, i.e. Θ_i lags Θ_{i-1}, g must be globally positive, in order to increase the frequency of pedestrian i, thus fostering synchrony with pedestrian $i-1$; similarly when $(\Theta_{i-1} - \Theta_i)$ is negative, i.e. Θ_i leads Θ_{i-1}, the term in question must be globally negative. Of course g must be periodic in $(\Theta_{i-1} - \Theta_i)$, and the simplest periodic function that satisfies these requirements is the sine function;
3. the constant of proportionality D_i measures the effect of the pedestrian $i-1$ on the following pedestrian i. Since D_i is the amplitude of the maximum phase shift corrections between walkers, it can be considered as a sort of 'visual sensitivity' of pedestrians to the crowd self-synchronization. Thus we will have $g = 0$ when $D_i = 0$, i.e. the pedestrians are visually insensitive. It is reasonable to consider a certain variation of visual perception among individuals in the population. We should in general use a random distribution D_i for these sensitivities, but lacking specific studies in this direction, we will later make the simplifying assumption that $D_i = D$, a single constant value for all walkers (similarly to what have been done for the C_i).

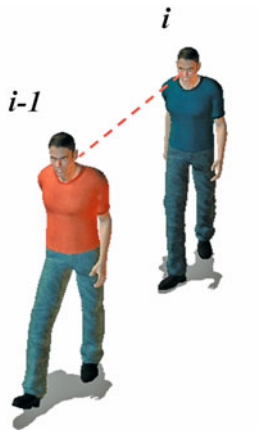

Fig. 23 Scheme of the visual pedestrian-to-pedestrian interaction

Hence with this model, when pedestrian i sees pedestrian $i-1$ walking near in front of him, he is visually influenced and he slows down or speeds up so as to walk more nearly in phase on the next step. This effect certainly contributes to speed up the trigger of the bridge first lateral movements. It is obvious that if the visual stimulus of the previous pedestrian $i-1$ is too fast or too slow, the pedestrian i cannot keep up and entrainment is lost. Therefore, this type of synchronization is certainly fostered in the case of a typologically homogeneous crowd, i.e. with a Gaussian distribution of native frequencies characterized by a small standard deviation (Fig. 10).

Moreover the synchronization between pedestrians is clearly possible only if the number of persons on the bridge is sufficiently large so that they are able to influence each other. For this reason our modification to SAMEO model applies only in case of yet crowded bridge, with a density over $0.6\,\mathrm{pers/m^2}$ [15] (corresponding to a relative distance between pedestrians of about 1 m or even less): over this density value the single pedestrian is no longer able to walk with his individual undisturbed step frequency and walking velocity. Within this limit, we have to detect the admissible scale range for D_i (i.e. to fix its lower and upper bounds) and to predict the effects of D_i on the model.

Some preliminary qualitative physical considerations allow affirming that:

1. D_i cannot be negative both for a physical reason related to its meaning, and because the sine function already controls, in the mathematically right way, the increase/decrease of the walking frequency due to 'self'-synchronization between pedestrians;
2. as the visual sensitivity D_i increases, we expect a decrease of the critical number N_c, because the 'self'-synchronization between pedestrians tends to facilitate the 'global' synchronization with the bridge;
3. large values of D_i could mean that each pedestrian is so much influenced by the previous one because of their minimal distance (crowd close to the densest possible packing) that he doesn't mind the bridge; namely the pedestrians could synchronize each other on a frequency different from the bridge native one, thus

the critical number N_c triggering the phenomenon can increase instead of decreasing. This is obviously a limit case.

On the basis of these qualitative physical considerations, $D_i = 0\,\mathrm{s}^{-1}$ can be assumed as a lower bound for the visual sensitivity parameter to the 'self'- synchronization.

In order to determine also an upper bound for D_i, hereafter we consider the Eq. (11) with $C = 0\ \mathrm{m}^{-1}\mathrm{s}^{-1}$, in order to deal with the effects of D on the model only. The system, for N pedestrians, is made of $N-1$ equations (note that the first pedestrian has not a person ahead him and so it is not involved in the 'self'- synchronization. It is just a leader of the crowd and its native frequency, $\dot{\Theta}_1 = \Omega_1 \neq 0$, constitutes an initial condition for the problem):

$$\begin{cases} \dot{\Theta}_2 = \Omega_2 + D_2 \sin(\Theta_1 - \Theta_2)\,, \\ \vdots \\ \dot{\Theta}_i = \Omega_i + D_i \sin(\Theta_{i-1} - \Theta_i)\,, \\ \vdots \\ \dot{\Theta}_N = \Omega_N + D_N \sin(\Theta_{N-1} - \Theta_N). \end{cases} \tag{12}$$

The fixed points, corresponding to steady-states or equilibriums of the system, are given by $\dot{\Theta}_i = 0$, $\forall\, i = 2,\ldots,N$. From a qualitative point of view this is the limit situation, when overcrowding is such that pedestrians are packed and therefore they are forced to stop: $\dot{\Theta}_i$ is nil and the maximum value of D_i is achieved (it is the upper bound we are looking for).

For the generic pedestrian i the solution for $\dot{\Theta}_i = 0$ provides:

$$-\frac{\Omega_i}{D_i} = \sin(\Theta_{i-1} - \Theta_i)\,. \tag{13}$$

We highlight that, in order to have the equilibrium position, the condition $\left|-\Omega_i/D_i\right| < 1$, i.e. $D_i > \Omega_i$, must be satisfied.

From (13) we have

$$\Theta_i = \Theta_{i-1} + \arcsin\frac{\Omega_i}{D_i}\,, \quad i = 2,\ldots,N\,. \tag{14}$$

The first term Θ_1^* in this chain of equalities (14) is known, as the first pedestrian is not influenced by anyone else on the bridge, while the second is visually influenced by the first and so on. Thus we determine in cascade the solution of the system (12): $(\Theta_2^*, \Theta_3^*, ..., \Theta_N^*)$; the Jacobian matrix $\mathbf{J}$ evaluated at that point is:

$$\mathbf{J} = \begin{bmatrix} -\mu_2 & 0 & 0 & \cdots & 0 \\ \mu_3 & -\mu_3 & 0 & & 0 \\ 0 & \ddots & \ddots & \ddots & \vdots \\ \vdots & \ddots & \mu_{N-1} & -\mu_{N-1} & 0 \\ 0 & \cdots & 0 & \mu_N & -\mu_N \end{bmatrix}, \quad \mu_i = D_i\sqrt{1 - \left(\Omega_i/D_i\right)^2}\,. \tag{15}$$

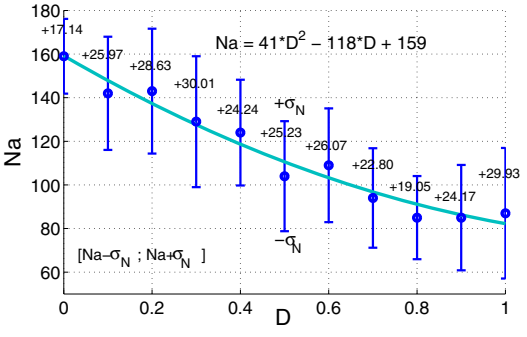

Fig. 24 Critical number of pedestrians versus D: data points, fitted quadratic curve and graphical display of the standard deviations associated to each mean value N_a

This matrix has negative eigenvalues $\lambda_i = -D_i\sqrt{1-(\Omega_i/D_i)^2}$, as it can be seen by inspection (remember that $D_i > \Omega_i$ otherwise the equilibrium solution does not exist); hence the fixed point $(\Theta_2^*, \Theta_3^*, ..., \Theta_N^*)$ is a stable node. In other words, as D_i increases, the phases tend towards those values $(\Theta_2^*, \Theta_3^*, \ldots, \Theta_N^*)$, equilibrium solutions of system (12). Therefore we infer that to not have the phenomenon of stable equilibrium, corresponding to overcrowding condition, we have to assume $D_i < \Omega_i$, and this constitutes an upper bound for D_i.

It is important to remark that from a physical point of view, for equilibrium of the system we mean the limit situation such that overcrowding is close to the densest possible packing and therefore it prevents any further form of motion: pedestrians are obliged to stop and their relative phases are blocked; the fixed point $(\Theta_2^*, \Theta_3^*, ..., \Theta_N^*)$ provides the pedestrian phases an instant before the packed configuration. This equilibrium is also stable, if nobody leaves the bridge. We impose that this equilibrium must be avoid because it is the upper possible limit for real situations; in this sense it allows an estimation of the maximum value for D_i: the maximum visual sensitivity threshold occurs when overcrowding is maximum.

For sake of simplicity, as already mentioned, D_i will be assumed constant, $D_i = D$, as it has been done with the other sensitivity parameter C (Sect. 2). Therefore, the bounds we have just found can be rewritten as $0 \leq D < \Omega_a = 1.03\,\mathrm{s}^{-1}$ (note that we refer to the mean of the Gaussian distribution of pedestrian lateral frequencies).

Afterwards we reintroduce $C = 16\,\mathrm{m}^{-1}\mathrm{s}^{-1}$ (original value from SAMEO model) in the governing equation (11), and we investigate values of D in the interval [0,1] s^{-1} in order to test the effects on the model. We obtain, as expected, a monotonically decreasing trend of the critical number of pedestrians triggering the synchronization versus D (Fig. 24).

We use once again the method of least squares to characterize data using a global fit; we obtain the following quadratic correlation function:

$$N_a = 41 \times D^2 - 118 \times D + 159\,. \tag{16}$$

In Fig. 24, for each group of simulations, we also report the standard deviation σ_N associated to the mean value N_a of the crowd critical number. We remark that for

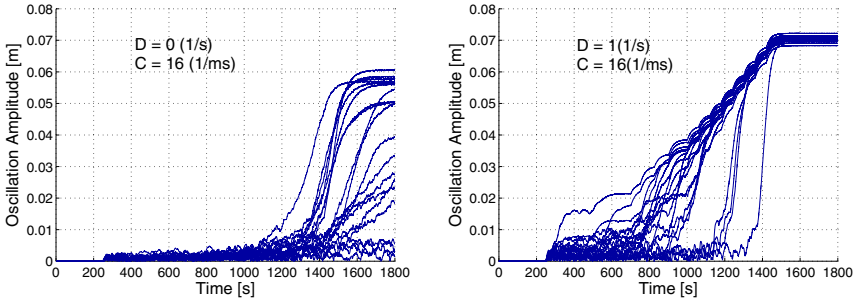

Fig. 25 Amplitude of vibration versus time: curves obtained with **a** $D = 0\,\mathrm{s}^{-1}$, $C = 16\,\mathrm{m}^{-1}\mathrm{s}^{-1}$ and with **b** $D = 1\,\mathrm{s}^{-1}$ and $C = 16\,\mathrm{m}^{-1}\mathrm{s}^{-1}$

$D = 0$ we are not actually considering pedestrian-to-pedestrian interaction and we fall back in the reference case, thus obtaining $N_a = 155$–160 and $\sigma_N = 27.7$–25.4; for $D = 1\,\mathrm{s}^{-1}$, we obtain a strongly reduced critical number $N_a = 85$ and $\sigma_N = 29.93$, being increased the pedestrian sensitivity to visual clues. The amplitude versus time curves for these two border cases are shown hereunder: Fig. 25a is the equivalent of Fig. 7, re-proposed to facilitate the comparison with Fig. 25b.

We note an increase of the final predicted amplitude of the bridge motion, which is, in any case, very close to the observed values on the Millennium Bridge.

It is evident, as expected, that this additional synchronization mechanism self-excites the phenomenon, as the critical threshold almost halves (from 155–160 to 85) with respect to the reference model.

2.2.8 Effects of the Two Synchronization Parameters C and D

When does the pedestrian-pedestrian visual interaction become irrelevant with respect to the interaction with the bridge lateral vibrations? How much N_a is influenced by C and D? Unfortunately these remain partly open questions, lacking a proper complementary experimental investigation.

The only thing we can do here is to perform a systematic numerical simulation aimed at determining the joint effect of C and D on the model critical threshold N_a. We report in Fig. 26 the contour plot of N_a as a function of C and D, which just permits understanding the joint effect of the synchronization parameters on the model behaviour.

This map is obtained by considering a grid of 12×11 points: each of them is the result of 200 simulations. The plot window is performed for D ranging in its definition interval $[0,1]\,\mathrm{s}^{-1}$ (see subsection 2.2.7), and for C varying in a restricted range of values, from $14\,\mathrm{m}^{-1}\mathrm{s}^{-1}$ up to $25\,\mathrm{m}^{-1}\mathrm{s}^{-1}$; this last choice is admissible in the light of the observations drawn in subsection 2.2.5.

Figure 26 highlights the complementarity of C and D in describing the phenomena. The simulations point out that as C and D increase, the critical number

decreases, according to common sense; moreover the same number N_a is obtained for smaller D when C is larger and vice versa. This trend has an intuitive physical confirmation; it is justified by the real difficulties pedestrians encounter when they walk on a laterally moving surface: as C increases, their sensory system, both neural and musculoskeletal, is so much involved in balance control that it does not care of the visual stimuli due to the presence of other people and the natural consequence is a lower D.

It is worthy of note that the two synchronization parameters, C and D, have different sensitivities, as we can see from their different scales of values (Fig. 26). By fixing one parameter and varying the other, if we increase D of $0.1\,\mathrm{s}^{-1}$ we obtain a decrease of N_a equal 10 pedestrians, but if we increase C of $0.1\,\mathrm{m}^{-1}\mathrm{s}^{-1}$ we obtain a decrease of N_a equal 1 (i.e. fixed the decrement of N_a, there is a ratio 10 : 1 in the increase of C with respect to D). In mathematical terms, we can affirm that the derivative of N_a with respect to C is smaller than the derivative of N_a with respect to D, although care must be used in this comparison because these are not dimensionless quantities. The direct consequence is that we have to pay more attention on the correct evaluation of the visual sensitivity parameter D.

Another aspect to take into account is that, by definition, the parameter C depends only on the pedestrians' sensitivity to the bridge lateral movements; however in the way it is used in the SAMEO model, actually it depends on the mode shape, even if, for sake of simplicity, only one value of C is considered for all the pedestrians on the bridge, independently of their position and distribution over the whole span. From a practical point of view its numerical value, as defined in the model, is acceptable only in the case of bridges having the same mode shape (sinusoidal) as the north span of the Millennium Bridge: for other bridges, C should be different. On the contrary, the parameter D, again by definition, depends only on the pedestrians' visual sensitivity to the motion of the people who are walking ahead, within a certain visual-psychological influence distance; therefore it is related to the crowd density and it can be estimated also through experiments with pedestrians walking on a fixed floor. Thus the numerical value of D is independent on the mode shape and it is valid for every bridge.

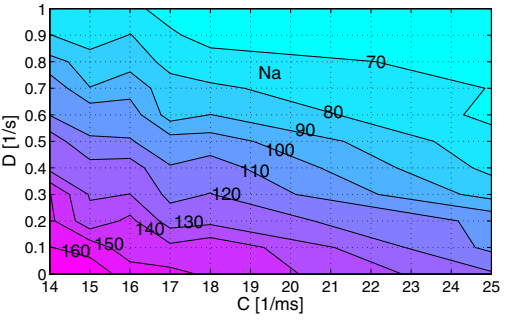

Fig. 26 Contour map for N_a obtained by varying C and D

In any case it is confirmed the need of tuning C and D through experimental tests, taking into account the simultaneous existence of the two synchronization degrees in relation to the crowd density and to the physical characteristics of the pedestrians involved (e.g., we expect that senior people or pedestrians with slight difficulties of locomotion are less prone to synchronize with the other persons, but are much more sensitive to the synchronization with the bridge). Once performed such tests, the contour plot in Fig. 26 could be a useful design map to evaluate N_a, depending on the expected predominant typology of pedestrian traffic.

2.2.9 Linear and Random Loading Paths

The reference (Arup's) loading path (Fig. 6a) is useful to detect the onset of the instabilities and to assess the model, but it is not general enough, and thus, for example, it is useless to design a control device. Here we study different, in particular *linear*, paths with the aim of investigating the variations of the critical threshold, and the effects of a larger number of pedestrians walking on the bridge.

It was estimated that between 80000 and 100000 people crossed the Millennium Bridge during the opening day, with a maximum of 2000 people on the deck at any time (approximately 450 only on the north span), resulting in a density of 1.3–1.5 persons/m^2 [12]. Observations on crowd indicate that the upper limit density for unconditioned free motion is only about 0.3 persons/m^2, while normal walking becomes practically impossible for densities above 1.7 persons/m^2 [54]. Therefore, in the following simulations, we arrive at a maximum of 550 ($= 1.7 \times 324$ square meters [12]) pedestrians walking simultaneously on the bridge (Fig. 27a). However it is important to mention that the number of pedestrians exciting the bridge is related to their distribution over the whole span, so that the local amplitude of the oscillation is related to the mode shape amplitude at that point, and thus it is a fraction of the amplitude of the excitation; moreover the theoretical limit numbers are for people who are walking, while usually some people will stop on the bridge, possibly contributing extra damping. This increases the practical critical threshold. Thus, we have competing phenomena practically reducing/increasing the theoretical critical threshold, and therefore our simulations have to be considered as a first, non systematic, study in this direction.

We consider five linear loading paths (Fig. 27) which differ in the number of pedestrians introduced on the bridge deck per unit time (we refer to it as 'loading velocity'); we identify them with a ramp factor, RF, defined as the inverse of their average slope. We obtain:

1. $RF = 0.5$, i.e. 10 ped/5 sec, $\rightarrow N_a = 240, \sigma_N = 34.98$;
2. $RF = 1$, i.e. 10 ped/10 sec, $\rightarrow N_a = 225, \sigma_N = 35.76$;
3. $RF = 3$, i.e. 10 ped/30 sec, $\rightarrow N_a = 190, \sigma_N = 36.21$;
4. $RF = 6$, i.e. 10 ped/60 sec, $\rightarrow N_a = 165, \sigma_N = 38.67$;
5. $RF = 12$, i.e. 10 ped/120 sec, $\rightarrow N_a = 160, \sigma_N = 39.00$.

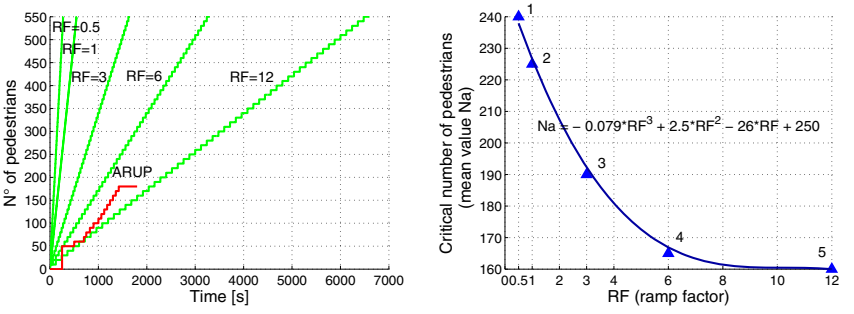

Fig. 27 Linear loading paths **a** and the corresponding crowd critical size **b**

For each of these RFs, the reported values of N_a and σ_N are, as usual, the results of 200 simulations. The best (in the least squares sense) cubic curve fitting the data is (Fig. 27b):

$$N_a = -0.079 \times RF^3 + 2.5 \cdot RF^2 - 26 \times RF + 250\,. \tag{17}$$

From Fig. 27 and from Eq. 17 we can understand and quantify the influence of the loading velocity on the instability threshold. For high loading velocities, i.e. low RF, the system has not enough time to develop synchronization. Pedestrians who enter the bridge will not be driven to adapt soon their footsteps to the slight motion of the structure: the crowd critical size rises. Instead, if we decrease the loading velocity, i.e. we consider high RF, when new pedestrians are introduced on the bridge, they will find a situation in which probably the bridge is already unstable and its wobbling is enough to force them to synchronize before the next load package arrives. So the critical threshold will be lower.

We also observe that the loading paths 4 (which, after the initial transient, has the same slope of the Arup's ramp) and 5 are characterized by a critical crowd size essentially identical; we can infer that by further decreasing the loading velocity likely the critical threshold no longer decreases (Fig. 27 b): Arup's critical threshold can be considered a lower bound of critical thresholds for other deterministic paths, thus being, in this respect, a conservative estimation.

We have also considered some *random* loading paths in order to test the general validity of the model. For each of the 4 groups of simulations summarized in Fig. 28, we have varied stochastically (inside fixed intervals) both the pedestrian increment and the time step. These intervals have been chosen in order to obtain, on average, loading paths comparable with those we have studied above. The numerical simulations give:

1. $RF_a = 1$, i.e. 5–15 pedestrians/5–15 sec (on average 10 ped/10 sec) $\rightarrow N_a = 184, \sigma_N = 22.29$;
2. $RF_a = 3$, i.e. 5–15 pedestrians/10–50 sec (on average 10 ped/30 sec) $\rightarrow N_a = 165, \sigma_N = 18.72$;

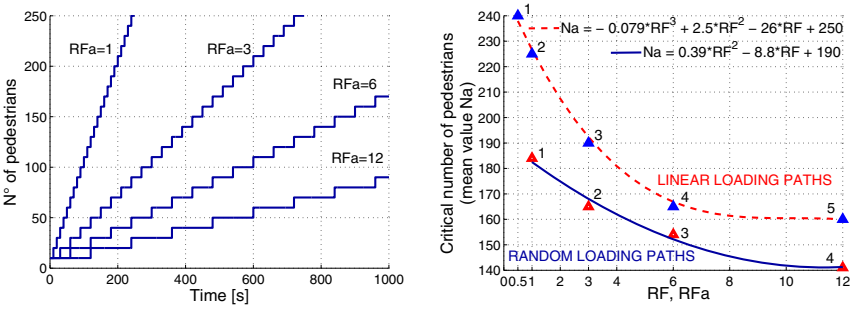

Fig. 28 Random loading paths (average trends) **a** and the corresponding crowd critical size **b**: comparison with the results from the linear loading paths

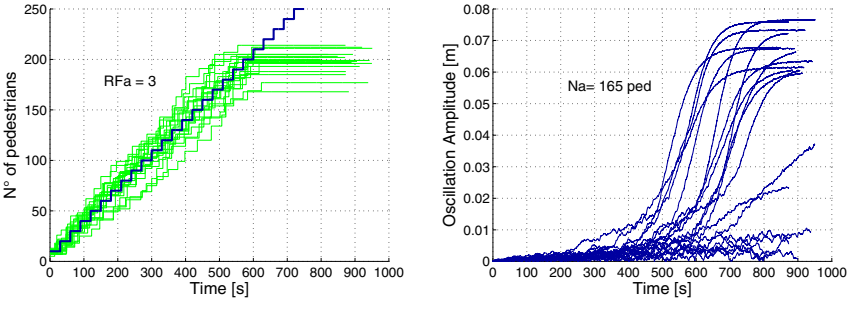

Fig. 29 Random loading paths with $RF_a = 3$ **a** and corresponding amplitude curves **b**

3. $RF_a = 6$, i.e. 5–15 pedestrians/40–80 sec (on average 10 ped/60 sec) $\rightarrow N_a = 154, \sigma_N = 21.49$;
4. $RF_a = 12$, i.e. 5–15 pedestrians/70–170 sec (on average 10 ped/120 sec) $\rightarrow N_a = 141, \sigma_N = 29.19$.

We use once again the method of least squares to characterize data using a global fit; we obtain the following quadratic correlation function (see Fig. 28b):

$$N_a = 0.39 \times RF_a^2 - 8.8 \times RF_a + 190\,. \tag{18}$$

We can observe that the decrease of N_a with RF, previously observed in deterministic ramps, is maintained, with the same qualitative behaviour. Passing from deterministic to stochastic ramps we observe a systematic decrease of the critical threshold of about 13% (Fig. 28b) which should be carefully considered by the designer. In any case the values obtained are in quite reasonable agreement both with the experimental and with the numerical results of the previous simulations.

It is interesting to show at least a sample of the output from our simulations, e.g. for $RF_a = 3$ (Fig. 29).

Despite the dispersion due to the randomness of the loading paths (Fig. 29a), the results are encouraging as the qualitative trend of the amplitude curves is maintained on average (Fig. 29b): the dynamic response of the bridge continues to be stable until a critical threshold and then increases rapidly towards a final landing. Furthermore, the predicted amplitude of the bridge motion is very close, on average, to the observed value of about 5–7 cm (see Fig. 29b). This is a remarkable robustness property of the SAMEO model, especially if we think to the many uncertainties which affect this type of problems.

3 A Discrete-Time Model

The critical overview of the existing literature, presented in Sect. 1, highlights many continuous-time models explaining the excessive lateral sway motion induced by a crowd crossing a footbridge. They are governed by partial or ordinary nonlinear differential equations (ODEs), and commonly cannot be solved in closed form but require extensive numerical simulations to be utilized in practice [52], as shown in the previous section. To overcome this drawback, in this second part of the chapter we present a nonlinear discrete-time model able to describe the synchronous lateral excitation without numerical simulations [27].

The basic idea is to work in the context of discrete dynamics, by an appropriate choice of a Poincaré section, thus turning a continuous dynamical system into a discrete one. If the Poincaré section is carefully chosen, no information is lost concerning the qualitative behavior of the dynamics [44].

Some approximations and simplifications are assumed in order to obtain a model which is as simple as possible and with the least possible number of parameters, while keeping the description of the underlying mechanical event. Some of these approximations can then be removed in order to have a model of more general validity. In spite of the approximations, however, the model is able to provide a reliable value of the number of pedestrians which trigger the synchronization, thus predicting the onset of instability which is also the onset of crowd synchronization.

From a dynamical system point of view, the main result is that the model highlights how the phenomenon can be seen as a perturbation of a classical pitchfork bifurcation, which is then shown to be the underlying dynamical event. It is worth to note that the proposed model is independent of the specific case of the Millennium Bridge, which is considered as a reference (Sect. 3.4), so it is applicable to any bridge where a similar problem is observed or expected to occur.

Besides improving the understanding of the physical phenomenon, our model proves simple and reliable in its previsions; therefore, it may be useful for estimating the damping needed to stabilize other exceptionally crowded footbridges against synchronous lateral excitations by pedestrians, or for designing other technologies aimed at eliminating the phenomenon in real structures.

3.1 Single Degree of Freedom Oscillator and Discrete Dynamic Model

According to the considerations made in Sect. 1, the dynamics of the bridge are governed by the Eq. (1). Introducing the quantities

$$t = \sqrt{\frac{M}{K}}\bar{t} = \frac{\bar{t}}{\Omega}, \quad X(t) = x(\bar{t}), \quad B = 2\sqrt{MK}\,\xi, \quad F_{ped}(t) = Kf(\bar{t}), \tag{19}$$

the Eq. (1) can be re-written in the dimensionless form:

$$\ddot{x} + 2\xi\dot{x} + x = f(\bar{t}), \tag{20}$$

where dots are derivatives with respect to the dimensionless time $\bar{t}$. In the following the hat is neglected for simplicity. Although equivalent, Eq. (20) is easier to be analyzed than (1) (it has less parameters), and thus it will be considered in the following.

3.1.1 Free Dynamics

In the unforced case $f(t) = 0$, the general solution of (20) is:

$$x(t) = c_1 e^{-\xi t}\sin\left(\sqrt{1-\xi^2}t\right) + c_2 e^{-\xi t}\cos\left(\sqrt{1-\xi^2}t\right), \tag{21}$$

so that $\omega = \sqrt{1-\xi^2}$ is the natural circular frequency and $p = 2\pi/\omega$ is the period, i.e. the time distance between two successive relative maximum points of the system motion.

We call x_n the amplitude of the generic relative maximum of the motion (see Fig. 30). We want to find an analytical relation, $x_{n+1} = l(x_n)$, between one peak and the subsequent in time. This map describes the so-called peak-to-peak dynamics (PPD) introduced by Lorenz in the study of chaos [10]. With this aim we assume that the starting point is a peak: $x(0) = x_n$ and $\dot{x}(0) = 0$. With these initial conditions we obtain:

$$x(t) = x_n e^{-\xi t}\left[\frac{\xi}{\sqrt{1-\xi^2}}\sin\left(\sqrt{1-\xi^2}t\right) + \cos\left(\sqrt{1-\xi^2}t\right)\right], \tag{22}$$

which is depicted in Fig. 30 for $\xi = 0.05$.

From Fig. 30 we can see that the successive peak occurs after one period. Thus, if we consider $x_{n+1} = l(x_n)$ we are actually considering a stroboscopic Poincaré map sampled at each period. We then have:

$$x_{n+1} = x(p) = x_n e^{\frac{-2\pi\xi}{\sqrt{1-\xi^2}}} = \alpha x_n, \tag{23}$$

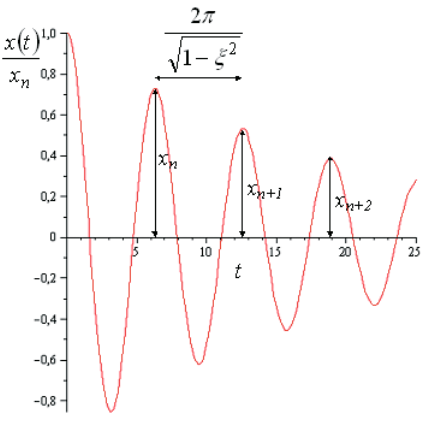

Fig. 30 The solution $x(t)/x_n$ of the damped harmonic oscillator with $\xi = 0.05$

where the parameter $\alpha \leq 1$ is defined by

$$\alpha = e^{-\frac{2\pi\xi}{\sqrt{1-\xi^2}}} \cong 1 - 2\pi\xi + \ldots . \tag{24}$$

Equation (23) is the simplest (it is linear) discrete-time dynamical system we are considering. We exclude the value $\alpha = 1$ because it corresponds to the unrealistic case of absence of damping. Its dynamic behavior is trivial: by iterating the map we obtain $x_n = \alpha^n x_0$, x_0 being the initial condition. Thus, all initial conditions tend, as expected, to the rest position $x = 0$.

3.1.2 Forced Dynamics: Single Pedestrian

We assume that a walking pedestrian acts as a periodic forcing on the oscillator. Here we idealize the pedestrian force as sinusoidal, even though experiments on a treadmill reveal a periodic trend more similar to a square wave (see Sect. 2.2.4). Practically, we consider the first term in the Fourier series expansion of the generic periodic function which approximates the experimental data concerning lateral walking forces on a still surface [41], [42], [8]:

$$f(t) = g \sin(\omega_p t + \phi) , \tag{25}$$

where:

1. $g > 0$ is the dimensionless force amplitude, such that $G = gK = 30\,\mathrm{N}$ on average [1]. G is the maximum lateral force exerted by a pedestrian. We remember that we are focusing on the lateral component of pedestrian forcing, the only one responsible for synchronous lateral excitation;
2. ω_p is the pedestrian footstep native frequency and $p_p = 2\pi/\omega_p$ his/her period;
3. $\phi \in [0, 2\pi]$ is the pedestrian temporal phase.

Substituting Eq. (25) into Eq. (20) we obtain the equation of motion for the case of single pedestrian:

$$\ddot{x} + 2\xi\dot{x} + x = g\sin(\omega_p t + \phi)\,. \tag{26}$$

The exact solution of Eq. (26), obtained with $x(0) = x_n$ and $\dot{x}(0) = 0$, calculated at $t = p$ (i.e. after one period) and then named x_{n+1} gives:

$$x_{n+1} = \alpha x_n + g\left[k_1\sin(\phi) + k_2\cos(\phi)\right], \tag{27}$$

where

$$\begin{aligned} k_1 &= \frac{(\omega_p^2-1)e^{\frac{-2\pi\xi}{\sqrt{1-\xi^2}}} + (1-\omega_p^2)\cos\left(\frac{2\pi\omega_p}{\sqrt{1-\xi^2}}\right) + 2\xi\omega_p\sin\left(\frac{2\pi\omega_p}{\sqrt{1-\xi^2}}\right)}{(1-\omega_p^2)^2 + 4\xi^2\omega_p^2}, \\ k_2 &= \frac{2\xi\omega_p e^{\frac{-2\pi\xi}{\sqrt{1-\xi^2}}} + (1-\omega_p^2)\sin\left(\frac{2\pi\omega_p}{\sqrt{1-\xi^2}}\right) - 2\xi\omega_p\cos\left(\frac{2\pi\omega_p}{\sqrt{1-\xi^2}}\right)}{(1-\omega_p^2)^2 + 4\xi^2\omega_p^2}. \end{aligned} \tag{28}$$

Defining:

$$\beta = g\sqrt{k_1^2+k_2^2},\quad \sin(\gamma) = \frac{k_1}{\sqrt{k_1^2+k_2^2}},\quad \cos(\gamma) = \frac{k_2}{\sqrt{k_1^2+k_2^2}}, \tag{29}$$

we can re-write Eq. (27) in the simpler form:

$$x_{n+1} = l(x_n) = \alpha x_n + \beta\cos(\phi - \gamma)\,. \tag{30}$$

Comparing Eq. (30) with Eq. (23), we see that the influence of the single pedestrian's motion on the map is described by the additional term on the right hand side.

We observe that if the pedestrian period is sufficiently close to the structure's natural period (i.e. $\omega_p \cong \omega$) it is possible a bridge-pedestrian interaction. In the worst-case scenario of perfect resonance, $\omega_p = \omega = \sqrt{1-\xi^2}$, it follows that:

$$\begin{aligned} k_1 &= \frac{1-e^{\frac{-2\pi\xi}{\sqrt{1-\xi^2}}}}{4-3\xi^2} = \frac{1-\alpha}{4-3\xi^2}, \\ k_2 &= -2\frac{\sqrt{1-\xi^2}}{\xi}\frac{1-e^{\frac{-2\pi\xi}{\sqrt{1-\xi^2}}}}{4-3\xi^2} = -2\frac{\sqrt{1-\xi^2}}{\xi}\frac{1-\alpha}{4-3\xi^2}, \\ \beta &= g\frac{1-e^{\frac{-2\pi\xi}{\sqrt{1-\xi^2}}}}{\xi\sqrt{4-3\xi^2}} = g\frac{1-\alpha}{\xi\sqrt{4-3\xi^2}},\quad \tan(\gamma) = -\frac{1}{2}\frac{\xi}{\sqrt{1-\xi^2}}. \end{aligned} \tag{31}$$

The problem becomes simpler, since being α and γ functions of ξ, the only parameters are ϕ, ξ and β (i.e. g). Furthermore, in this case, the peak-to-peak map corresponds to the stroboscopic Poincaré map.

Also in this case the dynamics of the (discrete) Eq. (30) are trivial. All initial conditions tend to the map fixed point

$$x = \frac{\beta \cos(\phi - \gamma)}{1 - \alpha}, \tag{32}$$

corresponding to a periodic oscillation of the real system. We have that $1 - \alpha = 2\pi\xi + \ldots$ is a small quantity, so that x is large, according to the fact that we are in (perfect) resonance.

3.1.3 Forced Dynamics: Crowd of Pedestrians

When a crowd of N pedestrians is walking on the bridge, the force is:

$$f(t) = \sum_{i=1}^{N} g_i \sin(\omega_{p,i} t + \phi_i), \tag{33}$$

where g_i is the lateral force exerted by the i^{th} pedestrian and $p_{p,i} = 2\pi/\omega_{p,i}$ is the natural period of his/her footstep; both are stochastic variables depending on the characteristics of the pedestrian himself. The pedestrian phase ϕ_i, still a stochastic variable, depends instead on the instant of time in which the pedestrian enters the bridge.

We consider a randomly walking crowd and we suppose a free entrance of pedestrians on the bridge. Therefore, ϕ_i is a stochastic variable uniformly distributed over its interval of existence $[0, 2\pi]$.

We instead introduce a simplification by assuming that all the pedestrians have the same native frequency, $\omega_{p,i} = \omega_p$. This assumption corresponds to the worst-case scenario, and actually occurs during synchronization because all the pedestrians tend to walk with the same period by feedback modifications to their native period, as shown by the SAMEO model in Sect. 2.

With the hypothesis $\omega_{p,i} = \omega_p$ the excitation Eq. (33) is a $(2\pi/\omega_p)$-periodic function, which can be re-written in the form:

$$f(t) = \bar{g} \sin\left(\omega_p t + \bar{\phi}\right), \tag{34}$$

with

$$\bar{g} = \sqrt{\left[\sum_{i=1}^{N} g_i \cos(\phi_i)\right]^2 + \left[\sum_{i=1}^{N} g_i \sin(\phi_i)\right]^2}, \quad \tan\left(\bar{\phi}\right) = \frac{\sum_{i=1}^{N} g_i \sin(\phi_i)}{\sum_{i=1}^{N} g_i \cos(\phi_i)}. \tag{35}$$

The expression (34) is formally similar to Eq. (25), so that we bring back the crowd's forcing to an *equivalent pedestrian's* force:

1. $\bar{g}$ is the overall lateral force amplitude due to crowd's motion;
2. $\bar{\phi}$ is the mean phase.

In the case of *perfectly synchronous* pedestrians, i.e. $\phi_i = \phi \pm 2n\pi$, the expressions (35) become:

$$\bar{g} = \sum_{i=1}^{N} g_i = N g_{average}\,, \quad \bar{\phi} = \phi\,. \tag{36}$$

In case of *perfectly asynchronous* pedestrians, i.e. for each pedestrian there is, on average, another with opposite phase, we have $\bar{g} = 0$.

Therefore $\bar{g}$ depends on the pedestrians' degree of synchronization, an observation which is crucial for the following developments.

Comparing Eq. (34) with Eq. (25), the map (30) becomes:

$$x_{n+1} = l(x_n) = \alpha x_n + \bar{\beta}\cos\left(\bar{\phi} - \gamma\right), \quad \bar{\beta} = \bar{g}\sqrt{k_1^2 + k_2^2}, \tag{37}$$

where k_1, k_2 and γ are unmodified.

The map (37) is formally identical to the previous one for single pedestrian.

Hereafter we will describe the crowd's force only by the parameters $\bar{g}$ (or $\bar{\beta}$), $\bar{\phi}$ and ω_p. If we further assume, as done for the single pedestrian, the worst-case scenario of perfect resonance $\omega_p = \omega = \sqrt{1-\xi^2}$, we then have only the two parameters $\bar{g}$ (or $\bar{\beta}$) and $\bar{\phi}$ describing the excitation acting on the bridge.

3.2 Interaction Oscillator-Pedestrians

In order to model the dynamical bridge-pedestrians interaction and to describe the natural tendency of the systems to synchronize, we must assume that they influence each other. Therefore, not only the motion amplitude x_n, but also the forcing characteristics $\bar{\beta}$ and $\bar{\phi}$ are assumed to vary on (discrete) time. Our state variables are then x_n, $\bar{\beta}_n$, $\bar{\phi}_n$, and Eq. (37) becomes:

$$x_{n+1} = \alpha x_n + \bar{\beta}_n \cos\left(\bar{\phi}_n - \gamma\right). \tag{38}$$

We note that the argument of the cosine function, $\sigma_n = \bar{\phi}_n - \gamma$, has a precise meaning in terms of synchronization:

1. when $\sigma_n = 0$, i.e. $\bar{\phi}_n = \gamma$, the crowd is perfectly synchronized with the bridge motion and the force exerted on the bridge is maximum;
2. when $\sigma_n = \pm\pi/2$, i.e. $\bar{\phi}_n = \gamma \pm \pi/2$, the crowd is perfectly asynchronous and the net force on the bridge is zero; this means that the crowd does not alter the bridge equilibrium state ($x = 0$) in this case.

On the basis of the previous observation we define σ_n to be the 'synchronization parameter'. Equation (38) takes the form:

$$x_{n+1} = \alpha x_n + \bar{\beta}_n \cos\left(\sigma_n\right), \tag{39}$$

and the system state variables are x_n, $\bar{\beta}_n$, σ_n.

The next step consists in finding the evolution laws for $\bar{\beta}_n$ and σ_n.

By noting that pedestrians tend to synchronize with the bridge lateral motion, we propose for σ_n the following evolution law:

$$\sigma_{n+1} = \frac{a}{a + x_n}\sigma_n \,, \tag{40}$$

where $a > 0$ is a parameter measuring the pedestrians' sensitivity to bridge lateral vibrations; it has the dimension of a length, and its value can be determined experimentally.

Equation (40) fulfils the following physical requirements which suggest its use:

1. the bridge-pedestrians system tends naturally to the maximally synchronous state. In fact $\lim_{n\to\infty} \sigma_n = 0$;
2. for small vibration amplitudes x_n, the pedestrians are not influenced by the bridge. In fact $\lim_{x_n\to 0} \sigma_{n+1} = \sigma_n$;
3. for large values of x_n, the pedestrians quickly synchronize, in fact $\lim_{x_n\to\infty} \sigma_n = 0$.

It is worth to note that Eq. (40) is susceptible of extension in order to obtain a more general theory. In fact, it is realistic to think that the synchronization is not asymptotically perfect; in mathematical terms, this means that $\lim_{n\to\infty} \sigma_n = \eta$ (η close but different from 0), or better, $\lim_{n\to\infty} \sigma_n = \Upsilon$, with Υ near but different from γ. We can introduce this aspect by simply substituting γ with Υ in the definition of σ_n.

As regards $\bar{\beta}_n$, its evolution law is known once we know the law for $\bar{g}_n$, being $\bar{\beta}_n = \bar{g}_n\sqrt{k_1^2 + k_2^2}$. Considering that $\bar{g}_n$ depends on the bridge-pedestrians synchronization level, we could relate it to the synchronization parameter σ_n and write $\bar{g}_n = \bar{g}_n(\sigma_n)$ such that:

1. if $\sigma_n = 0$, we should have $\bar{g}_n(0) = Ng_{average}$ (perfectly synchronous crowd);
2. if $\sigma_n = \pm\pi/2$, we should have $\bar{g}_n(\pm\pi/2) = 0$ (perfectly asynchronous crowd).

At the same time, it is also true that synchronization depends on the oscillation amplitude x_n. Therefore we can assert that $\bar{g}_n = \bar{g}_n(x_n)$, and in particular:

1. if the oscillation amplitude is nil, i.e. x_n = 0, we expect $\bar{g}_n(0) = 0$ (perfectly asynchronous crowd);
2. if the oscillation amplitude becomes large, $x_n \to \infty$, we expect $\bar{g}_n(x_n = \infty) = Ng_{average}$ (perfectly synchronous crowd). This is of course only a mathematical limit: from an engineering point of view we expect $\bar{g}_n \cong Ng_{average}$ even for finite, although 'large', values of x_n.

We observe that $\bar{g}_n(x_n)$ is a monotonically increasing function and it is easier to be 'invented' than $\bar{g}_n(\sigma_n)$. Therefore, we propose for $\bar{g}_n$ the following law which satisfies the aforementioned requirements:

$$\bar{g}_n = Ng_{average} \tanh\left(\frac{x_n}{\delta} + \varepsilon\right) . \tag{41}$$

$\delta > 0$ is a parameter with the dimensions of a length. It can be determined experimentally and it measures how fast the asymptotic value $Ng_{average}$ becomes saturated while the oscillations amplitude is growing up. δ can also represent the bridge displacement for which synchronization is almost completed, being $\tanh(1+\varepsilon) \cong 0.76 - 0.80$. As a consequence, its value can be estimated slightly lower than the bridge maximum lateral displacement.

$\varepsilon > 0$ is a perturbation/imperfection dimensionless parameter with respect to the limit ideal case $\varepsilon = 0$ (non-perturbed/perfect case) in which the bridge is still and the crowd is perfectly asynchronous and therefore unable to exert any lateral net force on the bridge itself. In real cases ($\varepsilon > 0$), even if the bridge is still, there is a certain component of lateral force due exclusively to random synchronization phenomena between pedestrians, which is assumed to be $Ng_{average}\tanh(\varepsilon)$ in this model. In general, however, this force is small, so that we assume ε to be small.

Substituting Eq. (41) into $\bar{\beta}_n = \bar{g}_n\sqrt{k_1^2 + k_2^2}$, we have:

$$\bar{\beta}_n = \sqrt{k_1^2 + k_2^2}\, N g_{average} \tanh\left(\frac{x_n}{\delta} + \varepsilon\right), \tag{42}$$

and we note that, with the previous assumptions, $\bar{\beta}_n$ is no longer an *independent* variable.

Summarizing the previous developments, we have found that our discrete-time model has only two independent variables, x_n and σ_n, and it is described by the two-dimensional map:

$$\begin{cases} x_{n+1} = f_1(x_n, \sigma_n) = \alpha x_n + (1-\alpha)\,\delta \dfrac{N}{N_{cr}} \tanh\left(\dfrac{x_n}{\delta} + \varepsilon\right) \cos(\sigma_n), \\ \sigma_{n+1} = f_2(x_n, \sigma_n) = \dfrac{a}{a + x_n}\sigma_n. \end{cases} \tag{43}$$

The parameter N_{cr} appearing in (43) is of great practical interest and it is defined by:

$$N_{cr} = \frac{(1-\alpha)\delta}{g_{average}\sqrt{k_1^2 + k_2^2}} \cong \frac{2\delta\xi}{g_{average}} = \frac{2\xi\,\delta\,K}{G_{average}}. \tag{44}$$

Equations (43) and (44) describe the phenomenon of synchronization of pedestrians' motion with the lateral vibrations of footbridges. Note that in this model we consider a global synchronization, without distinguishing between the two different levels of synchronization observed in practice [15]: bridge-pedestrian and pedestrian-to-pedestrian (see Sects. 2.2.7 and 2.2.8).

The model parameters are the damping ξ, the sensitivities a and δ, the imperfection ε, $g_{average}$ and, of course, the number N of pedestrians walking on the bridge.

3.3 Fixed Points

The dynamic aspects of the map (43) of interest for the present chapter are the fixed points

$$\begin{cases} x = f_1(x, \sigma) \\ \sigma = f_2(x, \sigma) \end{cases}, \tag{45}$$

which corresponds to oscillation of the original (physical) system, and their stability. They are investigated in the following by distinguish between the imperfect ($\varepsilon > 0$) and the perfect ($\varepsilon = 0$) cases.

3.3.1 The Imperfect Case

We consider first the real case $\varepsilon > 0$. In this case the system of equations (45) becomes

$$\begin{cases} (1-\alpha)x = (1-\alpha)\,\delta \frac{N}{N_{cr}} \tanh\left(\frac{x}{\delta} + \varepsilon\right) \cos(\sigma) \\ \sigma x = 0 \end{cases}. \tag{46}$$

The second equation of (46) admits two solutions which, inserted in the first equation, give two different solutions:

$$\text{A}) : \begin{cases} x = 0 \\ \sigma = \pm\frac{\pi}{2} \end{cases}, \quad \text{B}) : \begin{cases} \sigma = 0 \\ \frac{x}{\delta} = \frac{N}{N_{cr}} \tanh\left(\frac{x}{\delta} + \varepsilon\right) \end{cases}. \tag{47}$$

The two fixed points $(47)_{\text{A}}$ correspond to the condition of bridge in equilibrium (motionless), with perfect bridge-pedestrians de-synchronization. We guess they are only theoretical solutions, i.e. they are unstable.

The fixed point $(47)_{\text{B}}$ corresponds to perfect bridge-crowd synchronization with non-vanishing oscillations of the bridge. As we will see later, they are stable solutions and they are involved in the phenomenon of synchronous lateral excitation.

It is worth to note that the equilibrium points are independent of the pedestrian sensitivity parameter a; therefore we don't need to determine it experimentally, unlike other models present in the literature [12], [47]. This is a worthy aspect of our model. However, we expect that a will influence the rate of convergence towards the equilibrium solutions.

To discuss the stability of the fixed points Eq. (47), we evaluate the eigenvalues of the Jacobian matrix of the system (43):

$$\mathbf{J} = \begin{bmatrix} \frac{\partial f_1}{\partial x_n} & \frac{\partial f_1}{\partial \sigma_n} \\ \frac{\partial f_2}{\partial x_n} & \frac{\partial f_2}{\partial \sigma_n} \end{bmatrix}. \tag{48}$$

For the fixed points A the eigenvalues are both real:

$$\lambda_{1,2} = \frac{1}{2}\left\{1+\alpha \pm \sqrt{(1-\alpha)^2 + 2(1-\alpha)\delta\frac{\pi}{a}\frac{N}{N_{cr}}\tanh(\varepsilon)}\right\}$$
$$\cong 1 - \pi\xi \pm \pi\xi\sqrt{1+\frac{\delta}{a}\frac{N}{N_{cr}}\frac{\tanh(\varepsilon)}{\xi}}. \tag{49}$$

We observe that $\lambda_1 > 1$ and $\lambda_2 < 1$, being $\varepsilon > 0$; therefore the fixed points $(47)_{\mathrm{A}}$ are saddles, and unstable as expected.

In correspondence of the fixed point B, the Jacobian matrix is diagonal and the eigenvalues, both real, are:

$$\lambda_1 = \alpha + (1-\alpha)\frac{N}{N_{cr}}\frac{1}{\cosh^2\left(\frac{x}{\delta}+\varepsilon\right)} = \alpha + (1-\alpha)\left[\frac{N}{N_{cr}} - \left(\frac{x}{\delta}\right)^2\frac{N_{cr}}{N}\right],$$
$$\lambda_2 = \frac{a}{a+x}, \tag{50}$$

where x is the fixed point position, solution of the second equation of system $(47)_{\mathrm{B}}$. We observe that $\lambda_2 < 1$, while the condition $\lambda_1 < 1$ corresponds to the inequality:

$$\left(\frac{x}{\delta}\right)^2 > \frac{N}{N_{cr}}\left(\frac{N}{N_{cr}} - 1\right) \tag{51}$$

which is always satisfied. Therefore the solution $(47)_{\mathrm{B}}$ is always stable, as expected. It is shown in red (grey) in Fig. 31 for different values of the parameter ε.

3.3.2 The Perfect Case

Now we consider the unperturbed limit case $\varepsilon = 0$ and we determine likewise the fixed points of the map (43). Again, there are two types of solutions of (45):

$$\mathrm{A}): \begin{cases} x = 0 \\ \forall\sigma \end{cases}, \quad \mathrm{B}): \begin{cases} \sigma = 0 \\ \dfrac{x}{\delta} = \dfrac{N}{N_{cr}}\tanh\left(\dfrac{x}{\delta}\right) \end{cases}. \tag{52}$$

The solutions $(52)_{\mathrm{A}}$ are a manifold of fixed points non depending on the relative phase crowd-bridge. They are all the points of the straight line $x = 0$. In the presence of perturbations, $\varepsilon > 0$, they are reduced to the only two unstable fixed points $x = 0$, $\sigma = \pm\pi/2$ previously investigated.

The solutions $(52)_{\mathrm{B}}$ are a curve of fixed points consisting of two branches: $x = 0$ and another one, $N = N_{cr}(x/\delta)/\tanh(x/\delta)$, bifurcating from the previous one at $N = N_{cr}$. It is shown in blue (black) in Fig. 31.

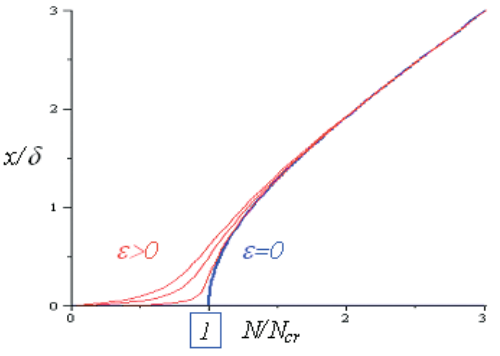

Fig. 31 Synchronized fixed points $x = x(N)$, for different values of parameter ε: $\varepsilon = 0.01,\ 0.05,\ 0.1$ (red (grey) curves); the solution for the unperturbed limit case $\varepsilon = 0$ is also shown (blue (black) curve)

To discuss the stability of the fixed points Eq. (52) we consider the eigenvalues of the Jacobian matrix (48). For the fixed points A the eigenvalues are real and equal to:

$$\lambda_1(\sigma) = \alpha + (1-\alpha)\frac{N}{N_{cr}}\cos(\sigma)\,, \quad \lambda_2 = 1\,. \tag{53}$$

Therefore, all the fixed points of the manifold are non-hyperbolic. As regards their stability, we can only affirm that they are certainly unstable when $|\lambda_1| > 1$, i.e., for

$$N > \frac{N_{cr}}{\cos(\sigma)},\ \text{for } \sigma \text{ such that } \cos(\sigma) > 0\,, \tag{54}$$

and

$$N > \frac{N_{cr}}{-\cos(\sigma)}\frac{1+\alpha}{1-\alpha},\ \text{for } \sigma \text{ such that } \cos(\sigma) < 0\,. \tag{55}$$

To further investigate the stability, we need to consider the nonlinear terms in the equations. We omit the computations, which are heavy and of little interest for our purposes; we show only the results, which are instead of great interest to improve the understanding of the physical event and to actually use our model. We find that:

1. all the fixed points $x = 0$ and $\sigma \neq 0$ are unstable;
2. the fixed point $x = 0$ and $\sigma = 0$ is stable for $N < N_{cr}$ and unstable for $N > N_{cr}$.

The eigenvalues of the fixed points B in Eq. (52) are given by Eq. (50) and thus they are both real and lesser than 1, so that the corresponding equilibrium position is always stable.

We can conclude that for $N = N_{cr}$, the bifurcating solution $(52)_B$ catches the stability of $x = \sigma = 0$ and triggers the lateral synchronization. This is a pitchfork bifurcation of degenerate type, as the fundamental branch is not made of hyperbolic points (blue (black) lines in Fig. 31).

On the basis of these observations, the fixed points $(47)_B$ can be seen as perturbations of the aforementioned pitchfork bifurcation.

The meaning of N_{cr}, as defined in Eq. (44) is now clear: it is the theoretical point where bifurcation occurs, the practical one being slightly smaller, as we can see from the lift-off point of the red (grey) curves in Fig. 31. It corresponds to the theoretical number of pedestrians triggering the synchronization and thus it is the most important information from an engineering point of view. Its relevance is underlined by the fact that it has a simple analytical formula, which helps in understanding how the various parameters influence the synchronization phenomenon.

In fact, Fig. 31 confirms that for small crowds, N/N_{cr} near zero, the amplitude ratio x/δ is near zero too, as walkers are desynchronized and randomly phased. Then, as more and more people walk on the deck, there is no hint of wide oscillations until the crowd reaches the critical size N_{cr}, after that wobbling and synchrony suddenly emerge simultaneously, as dual aspects of a single instability mechanism (Eq. (41) associates the synchronization with the current state of the oscillator).

3.4 A Case-Study: The London Millennium Footbridge

To test the agreement of our model with the dynamical behaviour of real structures we consider again as a benchmark the London Millennium Bridge, as it is the most well-known and well-documented case of 'lively' footbridge in the literature and in this sense it is the most suitable for a detailed analysis of the model behaviour and of the various aspects of the synchronous lateral excitation phenomenon.

With the data of the Millennium Bridge $M = 113000\,\text{kg}$, $B = 11000\,\text{kg/s}$, $K = 4730000\,\text{kg/s}^2$, $G_{average} = 30\,\text{N}$, $\xi = 0.0075$ and $g_{average} = G_{average}/K = 6.34 \times 10^{-6}\,\text{m}$ (see Sect. 2.1) we have from Eq. (44)

$$N_{cr} = \frac{2\delta\xi}{g_{average}} = 2365\delta\,. \tag{56}$$

Assuming $N_{cr} = 155$ (see Sect. 2.1) we obtain $\delta = 0.0654\,\text{m} = 6.5\,\text{cm}$; this means that the predicted amplitude of the bridge motion is very close to the observed values of about 5–7 cm on the opening day. There is a good agreement of the model results with the real behaviour of the bridge.

Another consideration can be drawn from Fig. 31 and from the second equation of the system $(47)_\text{B}$. They show that for large values of x and N the equation of the bifurcated branch becomes

$$x \cong \delta\frac{N}{N_{cr}}\,. \tag{57}$$

This linear trend is in good agreement with the SAMEO model results shown in Fig. 32, where the oscillations amplitude versus time curves have a similar linear trend in their final part. This observation allows a further estimate of the ratio δ/N_{cr}: with reference to Fig. 32 we register an amplitude of oscillation $x = 0.41\,\text{m}$ for $N = 1000$ pedestrians, namely, $\delta/N_{cr} = 4.1 \times 10^{-4}$. By assuming $N_{cr} = 155$, we obtain $\delta \cong 6.15\,\text{cm}$, which is comparable with the one previously calculated and confirms its reliability.

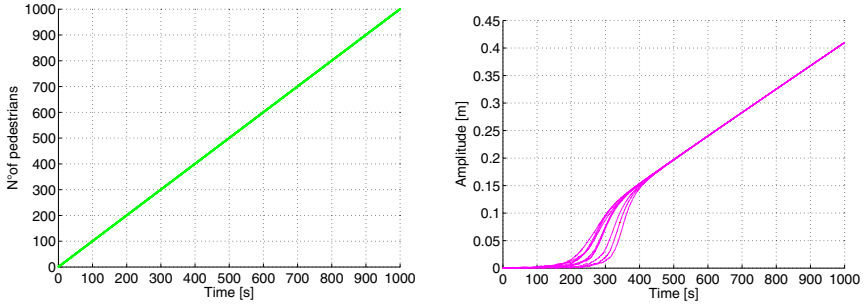

Fig. 32 Numerical results from the SAMEO model: **a** number of walkers on the bridge and **b** amplitude of vibration versus time. The various amplitude curves differ for the initial conditions randomly assigned to pedestrians' motion [30]

Comparing our equilibrium solutions (Fig. 31) with the SAMEO model results (Fig. 32), it is evident that our discrete-time model is able to describe accurately the phenomenon of synchronous lateral excitation, even with a simpler analytical formulation and, more important, without requiring numerical simulations.

4 Conclusions

After a focus on the problem of synchronous lateral excitation in slender footbridges and a critical overview of the existing literature on the topics, in the first section of this chapter a parametric study of the SAMEO model [47] for the pedestrians-induced lateral vibrations of footbridges has been performed and some modifications have been introduced and checked. The application of this model to the case of the London Millennium Bridge provides results in good agreement, both qualitatively and quantitatively, with observations and experiments. The model is able to predict simultaneously both the onset of bridge instability and the onset of crowd synchronization, providing a reliable value of the number of pedestrians which trigger the synchronization, i.e., the critical threshold. The steady state amplitude for bridge motion is also well predicted.

The extended numerical simulations permit to draw the following conclusions.

1. The initial distribution of pedestrians natural frequencies, i.e. their level of typological homogeneity, is decisive both for the trigger point of instability and for the temporal probability of the event to occur (see the relative time scales for onset of large bridge motion in Figs. 7, 9, 10) .
2. The shape of the pedestrian loading wave plays an important role. The ideal sinusoidal trend proposed in the original formulation of the model proves to be quite different from the typical time series of lateral forcing as measured by experiments on a treadmill [5]. The square-wave we introduce is more realistic and more conservative, as the critical number of pedestrians decreases.

3. The amplitude of lateral force due to pedestrians can increase dramatically when they change their gate on a moving platform. Numerical results, both for Abrams' relationship and for our bilinear relationship $G(A)$, show the necessity to consider this phenomenon. In fact, it affects the steady-state amplitude of the bridge motion and the speed at which the large amplitude oscillations set up. In particular, our relationship provides a lower critical number of pedestrians. Both the relationships share the same qualitative behaviour of the bridge-crowd system in terms of amplitude versus time curves.
4. The additional pedestrian-to-pedestrian synchronization self-excites the phenomenon, and accordingly the critical threshold considerably reduces. Although the two considered types of synchronization are different in their nature, they usually happen simultaneously and lead to the same result: an increase in the response of the structure. It is clear the necessity to take into account both of them.
5. Different loading paths (i.e. different numbers of pedestrians introduced on the bridge deck per unit time) affect both the time-history of the event and the critical number N_c. However, the phenomenon remains unaltered in its essence, thus emphasizing the robustness of the model.

It is worthy to note that the model depends only on the modal characteristics of the bridge, on the biological dynamics of human walking in a crowd, and on its dynamical interaction with the deck. So, unlike other models described in the literature [12], [11], [33], it is applicable to any bridge where a similar phenomenon is observed or expected to occur. The unique 'weak' point is the determination of the two parameters C (originally introduced to measure pedestrian sensitivity to bridge lateral oscillations) and D (we introduce here to measure the visual sensitivity to the synchronization between a pedestrian and the previous one). However the generality of the model is not invalidated as actual distributions of C and D could be determined through an *ad hoc* experimental campaign on a representative sample of the population. Experiments in this sense would be welcome.

Finally, it is necessary to remark that the SAMEO model is pseudo-stochastic, and it does not consider various (minor in our opinion) aspects. The perfect periodicity of the lateral human-induced load is assumed only with respect to the pedestrians phases (initially randomly assigned), as walking is not a perfectly periodic activity with respect to time, as wide experimental studies confirm [41], [42]; but the adopted approach is deterministic in its evolution and it can be criticized due to the random nature of walking forces, which would suggest the use of a really stochastic approach. Furthermore subharmonic or superharmonic resonances are not considered in the model.

All the previous observations, besides improving the understanding of the underlying physical phenomenon, allow us to state that the SAMEO model, despite some limitations, is sufficiently simple and robust in its previsions; therefore it may prove useful to estimate, e.g., the damping needed to stabilize other exceptionally crowded footbridges against synchronous lateral excitation by pedestrians. In this sense, it could constitute the basis to look for technical solutions aimed at limiting or avoiding the phenomenon of the pedestrians-induced lateral vibrations of footbridges.

As regards to the second section of this chapter, which is dedicated to the analysis of the discrete-time model, the most important conclusions are summarized in the following.

1. Also the proposed discrete-time model is independent of the specific real case-study we have considered (i.e. the London Millennium Bridge). It depends only on the modal characteristics of the bridge, on the biological dynamics of human walking in a crowd, and on its dynamical interaction with the deck.
2. As regards the parameters ε and δ , they do not limit neither the generality of the model nor its easiness and speed of application. In fact ε should be determined experimentally, but its evaluation pertains exclusively the unconstrained human walking dynamics (random synchronization phenomena) and not the footbridge we are studying. δ is a value very close to the bridge maximum lateral displacement and so we usually fix it in stage of project.
3. The stochastic aspects are put into account in the definition of the so-called 'equivalent pedestrian' which resumes the characteristics of the pedestrians in crowd, in terms of maximum exerted force, native frequency and random phase.
4. We assume that all the pedestrians have the same native frequency, even though experiments on a statistical sample of the population reveal a Gaussian distribution [54]. This is not a real problem, because our assumption constitutes only an analytical simplification which doesn't influence the structure of the model and its general validity.
5. Perfect periodicity of the lateral human-induced load is assumed. Actually, the walking force is not perfectly periodic and it could be attenuated due to interaction between the pedestrian and the structure. Moreover, we idealize again the pedestrian forcing as sinusoidal, even if experiments on a treadmill reveal a trend more similar to a square wave [5], as said.

The simple discrete-time model (2D map) is able to explain the main characteristics of the phenomenon of synchronous lateral excitation, without numerical simulations.

A simple analytical formula to compute the critical number of pedestrians triggering the synchronization is proposed. Its application to a real case-study returns reliable values, in good agreement both qualitatively and quantitatively with other consolidated results [30] and with observations [12]. Moreover it shows that N_{cr} depends only on the bridge damping and stiffness, on the average maximum lateral force exerted by walking pedestrians and then on the bridge maximum lateral displacement.

The main result, from a dynamical system point of view, is that the model highlights how the phenomenon is a perturbation of a classical (but degenerate) pitchfork bifurcation, which is the underlying dynamical event. This observation permits an improved understanding of the physical event underlying synchronization.

Finally, we can conclude that by the combined use of continuous- and discrete-time models we achieved a good understanding of the synchronization induced large lateral oscillations of footbridges, and reliable estimations of the triggering number of pedestrians.

References

1. Abrams, D.M.: Two coupled oscillator models: the Millennium Bridge and the chimera state. PhD Dissertation in Theoretical and Applied Mechanics, Cornell University, Ithaca, NY (2006), http://www.mit.edu/ dmabrams/papers/ Abrams_Daniel_Michael_dissertation.pdf (accessed September 28, 2008)
2. Arup videos (2000), http://www.arup.com/MillenniumBridge/indepth/video.html (accessed September 28, 2008)
3. Balthazar, J.M., Mook, D.T., Webwe, H.I., Brasil, R.M.L.R.F., Fenili, A., Belato, D., Felix, J.L.P.: An overview on non-ideal vibrations. Meccanica 38, 613–621 (2003)
4. Bauby, C.E., Kuo, A.D.: Active control of lateral balance in human walking. J. Biomech. 33, 1433–1440 (2000)
5. Belli, A., Bui, P., Berger, A., Geyssant, A., Lacour, J.R.: A treadmill ergometer for three-dimensional ground reaction forces measurement during walking. J. Biomech. 34(1), 105–112 (2001)
6. Blanchard, J., Davies, B.L., Smith, J.W.: Design criteria and analysis for dynamic loading of footbridges. In: Symposium Dyn Behav Bridges, Crowthorne, Berks, TRRL SR275:90-107 (1977)
7. Blekherman, A.N.: Autoparametric Resonance in a Pedestrian Steel Arch Bridge: Solferino Bridge. Paris. J. Bridge Eng. ASCE 12(6), 669–676 (2007)
8. Bodgi, J., Erlicher, S., Argoul, P.: Lateral vibration of footbridges under crowd-loading: Continuous crowd modelling approach. Key Eng. Mater. 347, 685–690 (2007)
9. Borri, C., Höffer, R.: Aeroelastic wind forces on flexible bridge girders. Meccanica 35, 1–15 (2000)
10. Candaten, M., Rinaldi, S.: Peak-to-peak dynamics: a critical survey. Int J. Bif. Chaos 10(8), 1805–1819 (2000)
11. Danbon, F., Grillaud, G.: Dynamic behaviour of a steel footbridge. Characterization and modelling of the dynamic loading induced by a moving crowd on the Solferino Footbridge in Paris. In: Proc Footbridge 2005 (2005)
12. Dallard, P., Fitzpatrick, A.J., Flint, A., Le Bourva, S., Low, A., Ridsdill Smith, R.M., Willford, M.: The London Millennium Footbridge. Struct. Eng. 79(22), 17–33 (2001)
13. Dallard, P., Fitzpatrick, A.J., Flint, A., Low, A., Ridsdill Smith, R.M., Willford, M., Roche, M.: London Millennium Bridge: pedestrian-induced lateral vibration. J. Bridge Eng. 6(6), 412–417 (2001)
14. Eckhardt, B., Ott, E., Strogatz, S.H., Abrams, D.M., McRobie, A.: Modeling walker synchronization on the Millennium Bridge. Phys. Rev. E 75, 021110 (2007)
15. Fib: Guidelines for the design of footbridges. Guide to good practice. Bulletin 32 (2005)
16. Fitzpatrick, A.J., Dallard, P., Le Bourva, S., Low, A., Ridsdill Smith, R.M., Willford, M.: Linking London: The Millennium Bridge. Royal Academy of Engineering, 1–28 (2001)
17. Fujino, Y., Pacheco, B.M., Nakamura, S.I., Warnitchai, P.: Synchronization of human walking observed during lateral vibration of a congested pedestrian bridge. Earthq. Eng. Struct. Dyn. 22, 741–758 (1993)
18. Gallagher, D.P.: Multi-Dimensional Optimization. Numer. Anal. 92, 563 (2006)
19. Gregoriou, G.G., Gotts, S.J., Zhou, H., Desimone, R.: High-Frequency, Long-Range Coupling Between Prefrontal and Visual Cortex During Attention. Science 324, 1207–1210 (2009)

20. Grundmann, H., Kreuzinger, H., Schneider, M.: Dynamic calculations of footbridges. Bauingenieur 68, 215–225 (1993)
21. Hughes, R.L.: A continuum theory for the flow of pedestrians. Transp. Res. Part B: Methodol. 36(6), 507–535 (2002)
22. Hof, A.L., Gazendam, M.G.J., Sinke, W.E.: The condition for dynamic stability. J. Biomech. 38, 1–8 (2005)
23. Hof, A.L., van Bockel, R.M., Schoppen, T., Postema, K.: Control of lateral balance in walking: experimental findings in normal subjects and above-knee amputees. Gait Posture 25, 250–258 (2007)
24. Hoogendoorn, S.P., Bovy, P.H.L.: Pedestrian route-choice and activity scheduling theory and models. Transp. Res. Part B: Methodol. 38(2), 169–190 (2004)
25. Kaneoke, Y.: Magnetoencephalography: In search of neural processes for visual motion information. Progr. Neurobiol. 80(5), 219–240 (2006)
26. Lagarias, J.C., Reeds, J.A., Wright, M.H., Wright, P.E.: Convergence Properties of the Nelder-Mead Simplex Method in Low Dimensions. SIAM J. Optim. 9(1), 112–147 (1998)
27. Lenci, S., Marcheggiani, L.: A discrete-time model for the phenomenon of synchronous lateral excitation due to pedestrians motion on footbridges. In: Proc. Third International Conference Footbridge 2008, Porto, Portugal (2008)
28. Macdonald, J.H.G.: Lateral excitation of bridges by balancing pedestrians. Proc. R. Soc. A 465, 1055–1073 (2009)
29. Matsumoto, Y., Nishioka, T., Shiojiri, H., Matsuzaki, K.: Dynamic design of footbridges. In: Proc. IABSE, Zurich, Switzerland (1978)
30. Marcheggiani, L., Lenci, S.: On a model for the pedestrians-induced lateral vibrations of footbridges. Meccanica 45, 531–551 (2010); doi:10.1007/s11012-009-9269-0
31. McRobie, A., Morgenthal, G., Lasenby, J., Ringer, M.: Section model tests on human-structure lock-in. Bridge Eng. 156(2), 71–79 (2003)
32. Mondada, L.: Emergent focused interactions in public places: A systematic analysis of the multimodal achievement of a common interactional space. J.Pragmat. 41(10), 1977–1997 (2008)
33. Nakamura, S.: Model for lateral excitation of footbridges by synchronous walking. J. Struct. Eng. ASCE 130, 32–37 (2004)
34. Nakamura, S.I., Kawasaki, T.: Lateral vibration of footbridges by synchronous walking. J. Constr. Steel Res. 62, 1148–1160 (2006)
35. Newland, D.E.: Vibration: problem and solution. In: Sudjic, D. (ed.) Blade of light: the story of London's Millennium Bridge. Penguin Books, London (2001)
36. Newland, D.E.: Pedestrian excitation of bridges - recent results. In: Proc. Tenth Int. Congr. Sound Vib., Stockholm, Sweden (2003)
37. Piccardo, G., Tubino, F.: Parametric resonance of flexible footbridges under crowd-induced lateral excitation. J. Sound Vib. 311, 353–371 (2008)
38. Roberts, T.M.: Lateral pedestrian excitation of footbridges. J. Bridge Eng. ASCE 10(1), 107–112 (2005)
39. Roberts, T.M.: Synchronised pedestrian lateral excitation of footbridges. In: Proc. Eurodyn 2005, pp. 1089–1094 (2005)
40. Roberts, T.M.: Probabilistic pedestrian lateral excitation of bridges. Proc. ICE, Bridge. Eng. 158(2), 53–61 (2005)
41. Ricciardelli, F., Pizzimenti, A.D.: Lateral Walking-Induced Forces on Footbridges. J. Bridge Eng. ASCE 12(6), 677–688 (2007)
42. Ricciardelli, F., Pizzimenti, A.D.: Experimental evaluation of the dynamic lateral loading of footbridges by walking pedestrians. In: Proc. Eurodyn. 2005 (2005)

43. Salvatori, L., Spinelli, P.: A discrete 3D model for bridge aerodynamics and aeroelasticity: nonlinearities and linearizations. Meccanica 42, 31–46 (2007)
44. Strogatz, S.H.: Nonlinear Dynamics and Chaos, with Applications to Physics, Biology, Chemistry, and Engineering. Perseus Books, Massachusetts (2000)
45. Strogatz, S.H.: Sync: the emerging science of spontaneous order. Hyperion, New York (2003)
46. Strogatz, S.H.: From Kuramoto to Crawford: exploring the onset of synchronization in populations of coupled oscillators. Physica D 143, 1–20 (2000)
47. Strogatz, S.H., Abrams, D.M., McRobie, F.A., Eckhardt, B., Ott, E.: Crowd synchrony on the Millennium Bridge. Nature 438, 43–44 (2005)
48. Sétra, Footbridges: assessment of vibrational behaviour of footbridges under pedestrian loading. Afgc, Paris (2006), `http://www.setra.equipement.gouv.fr/IMG/pdf/US_0644A_Footbridges.pdf` (accessed September 28, 2008)
49. Trovato, A., Erlicher, S., Argoul, P.: A modified Van der Pol oscillator for modelling the lateral force of a pedestrian during walking. In: Proc. Conference Vibrations, Chocs & Bruit, Lyon, France (2008)
50. Vaughan, C.L.: Theories of bipedal walking: an odyssey. J. Biomech. 36, 513–523 (2003)
51. Venuti, F., Bruno, L.: Crowd-structure interaction in lively footbridges under synchronous lateral excitation: A literature review. Physics of Life Reviews 6, 176–206 (2009)
52. Venuti, F., Bruno, L., Bellomo, N.: Crowd dynamics on a moving platform: Mathematical modelling and application to lively footbridges. Math. Comput. Model. 45, 252–269 (2007)
53. Wheeler, J.E.: Pedestrian induced vibration in footbridges. Technical Rep N°15, Main Roads Dep., Western Australia (1980)
54. Zivanovic, S., Pavic, A., Reynolds, P.: Vibration serviceability of footbridges under human-induced excitation: a literature review. J. Sound Vib. 279, 1–74 (2005)